Excitation and Ionisation in High Energy Density Plasmas

Steven Rose
Imperial College London
University of Oxford, UK

Overview

• Laser-produced plasmas can produce the highest laboratory thermal radiation fields (i.e. excluding laser fields).

• We consider in these lectures the direct effect of those radiation fields on the excitation and ionisation of high energy density plasmas (not the indirect effect of heating by the radiation field).

• We describe the theory describing excitation and ionisation in HED plasmas, particularly the contribution from the radiation field.

• We discuss experiments which test models with little or no radiation field, with a narrow-band radiation field and with a broad-band radiation field.

• We finish with some recent work that links laboratory HED plasmas with astrophysical plasma physics and spectroscopy.

• Conclusions

(energy in a Planckian radiation field)/(total energy)

$$\varepsilon_{energy} = \frac{aT^4}{\rho C_V T + aT^4}$$

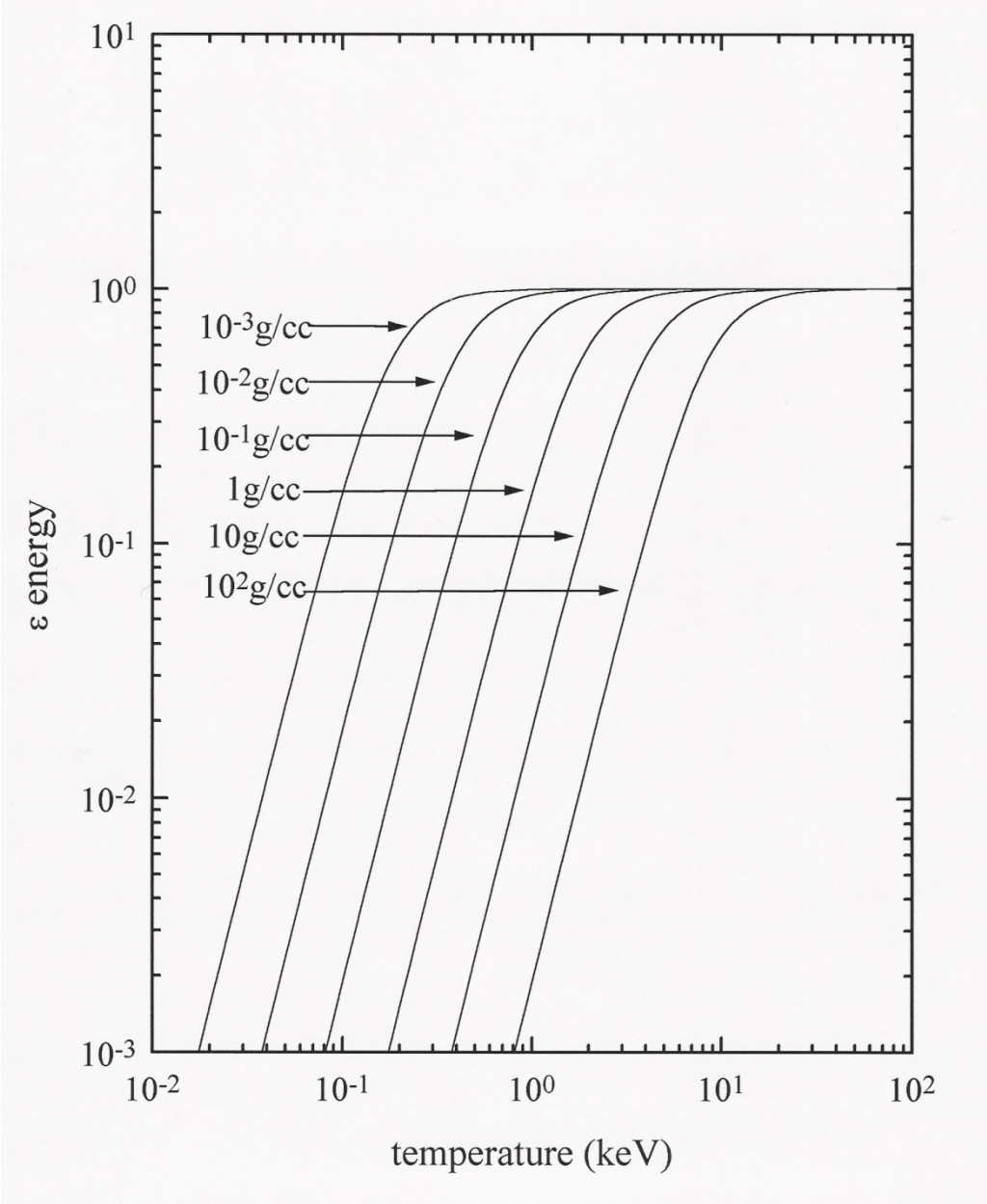

(pressure from a Planckian radiation field)/(total pressure)

$$\varepsilon_{pressure} = \frac{P_{rad}}{P_{mat} + P_{rad}}$$

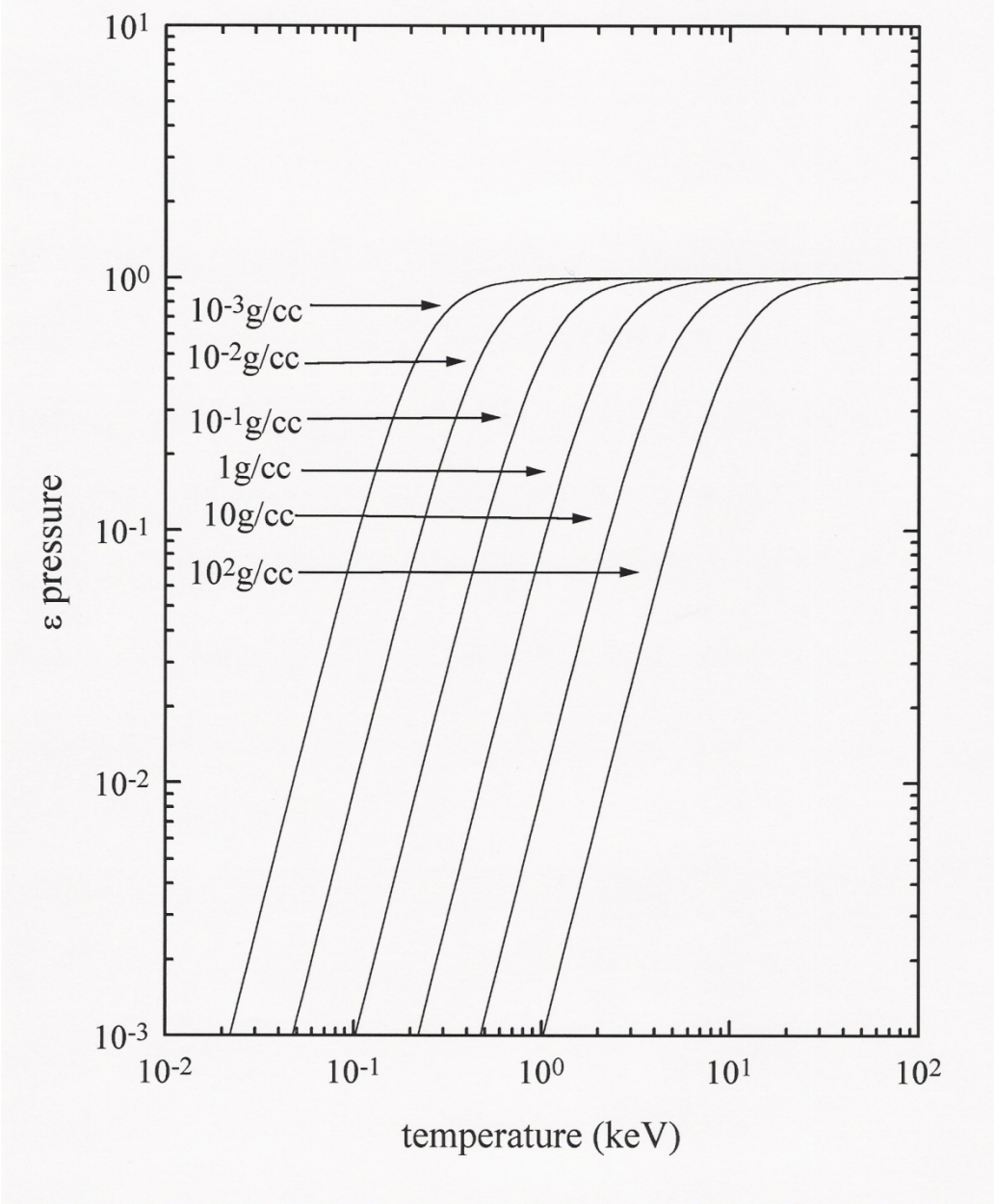

Radiation interacts with bound electrons through free electrons

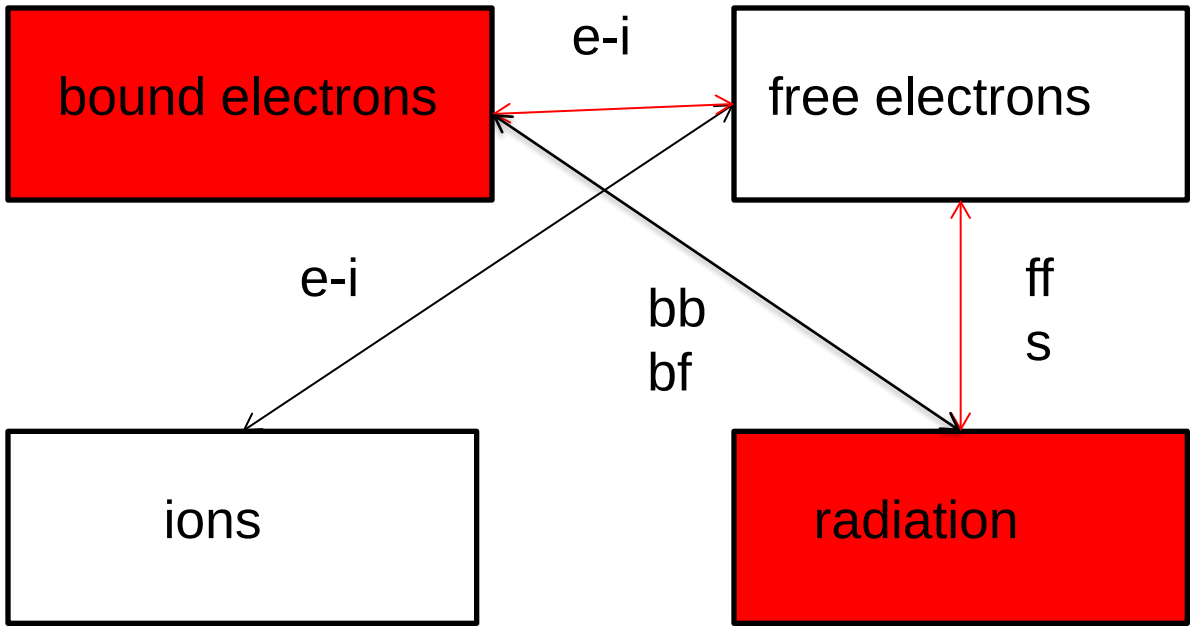

Radiation interacts with bound electrons directly

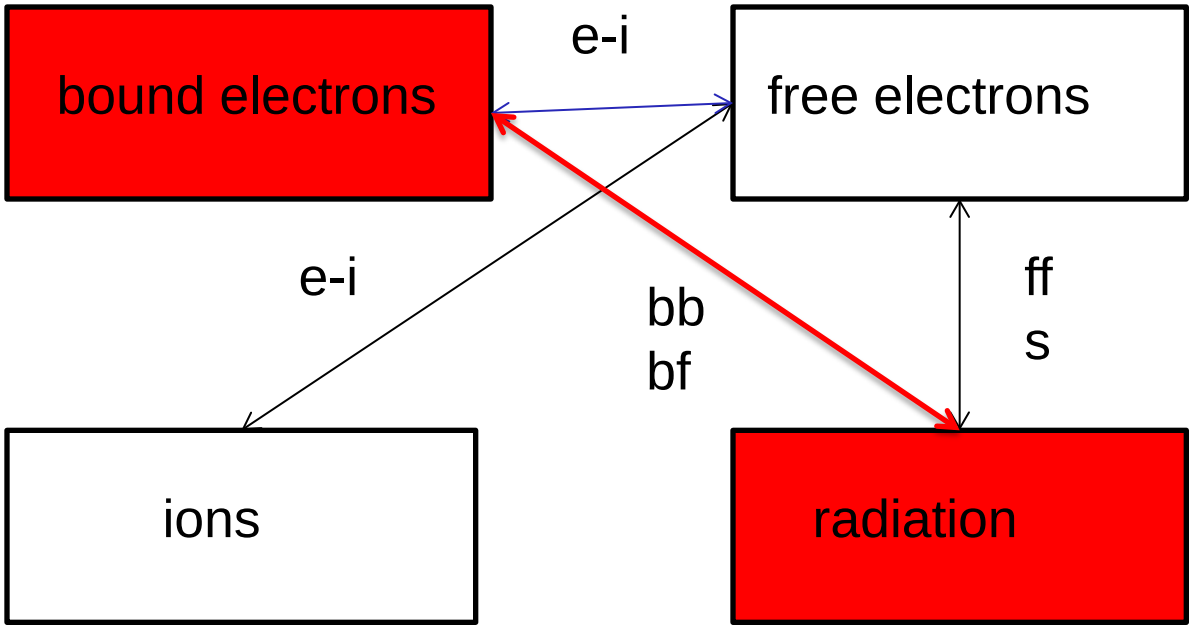

Collisional and radiative rates

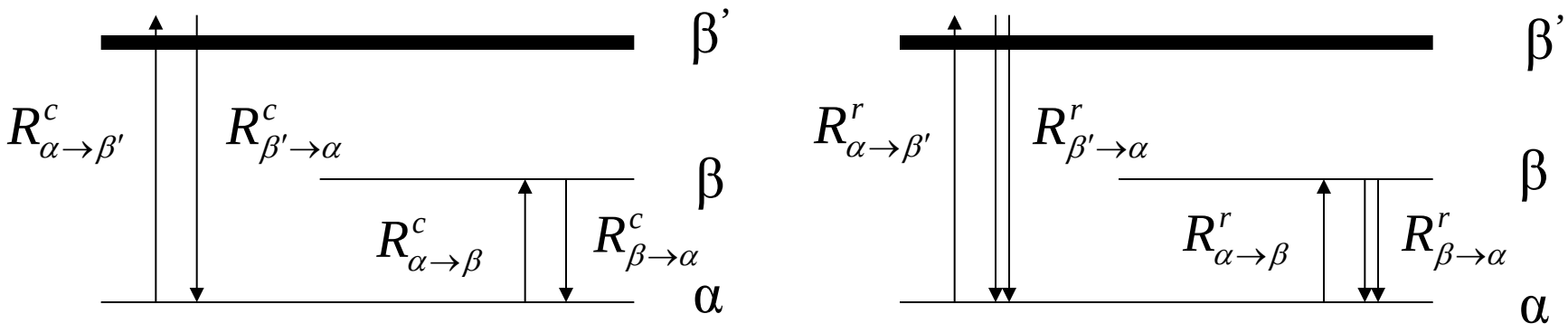

Collisional rates

$R^{c}_{\alpha\rightarrow\beta}$ Electron collisional excitation (~n_e)

$R^{c}_{\beta\rightarrow\alpha}$ Electron collisional de-excitation (~n_e)

$R^{c}_{\alpha\rightarrow\beta'}$ Electron collisional ionisation (~n_e) + Autoionisation

$R^{c}_{\beta'\rightarrow\alpha}$ Three-body recombination (~n_e^2) + Dielectronic recombination (~n_e)

Radiative rates

$R^r_{\alpha\to\beta}$ Photoexcitation - stimulated absorption

$R^r_{\beta\to\alpha}$ Photo de-excitation – spontaneous and stimulated emission

$R^r_{\alpha\to\beta'}$ Photoionisation – stimulated absorption

$R^r_{\beta'\to\alpha}$ Photorecombination (~n_e) – spontaneous and stimulated emission

Level of detail describing atomic states

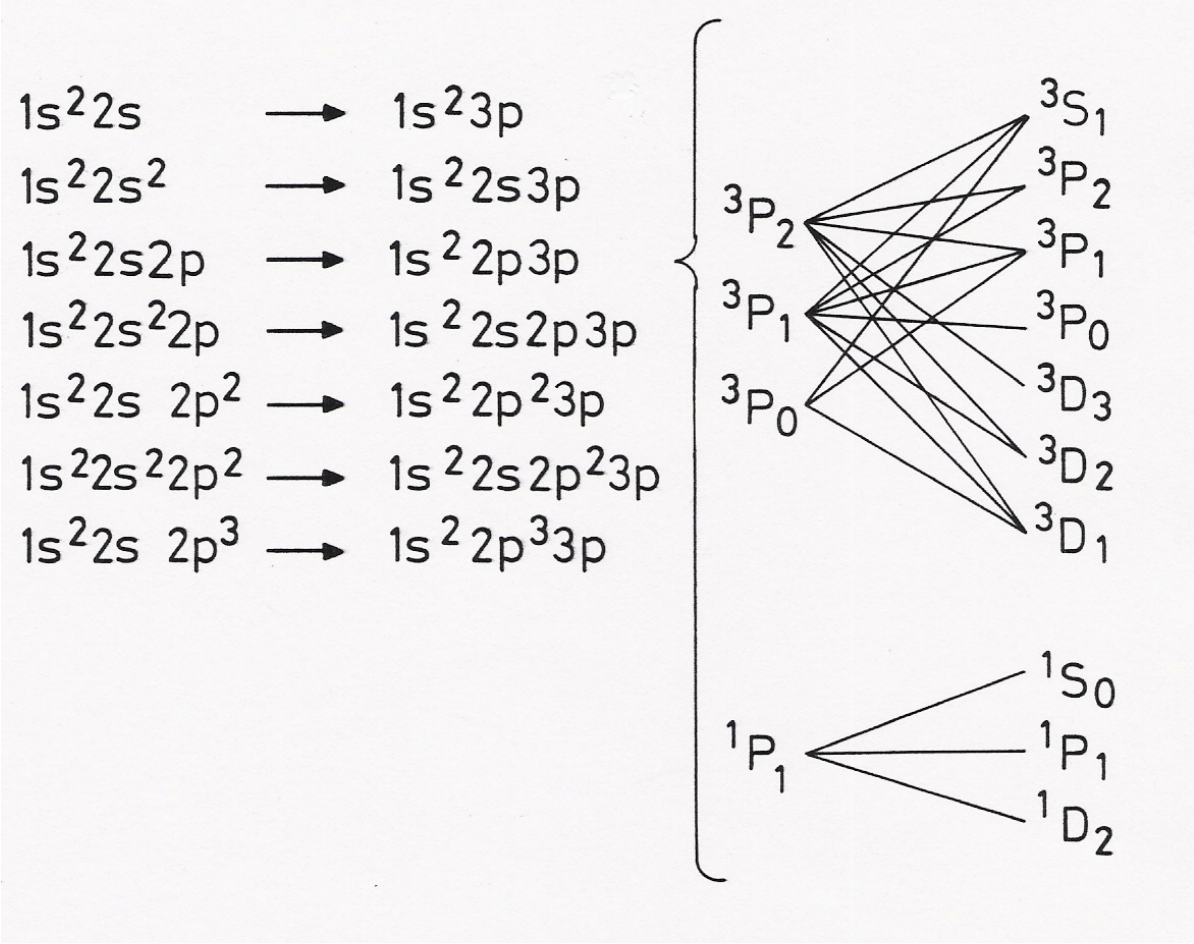

Detailed Configuration Accounting
DCA

Detailed Term Accounting
DTA

Rate equations

The rate equations governing the populations are for each level α

$$\frac{dn_\alpha(t)}{dt} = -n_\alpha(t)\sum_\beta (R^c_{\alpha\to\beta} + R^r_{\alpha\to\beta}) + \sum_\beta n_\beta(t)(R^c_{\beta\to\alpha} + R^r_{\beta\to\alpha})$$

which have the constraint

$$\sum_\alpha Z_\alpha(t) n_\alpha(t) = n^e$$

and for the case of the system having come to a steady-state

$$\frac{dn_\alpha(t)}{dt} = 0$$

Photo excitation / de-excitation rates

Both rates involve an integral over the line shape and the radiation field

$$R^{r}_{\alpha\to\beta} = 4\pi\int_{0}^{\infty}(\sigma_{\alpha\to\beta}(\nu)I(\nu)/h\nu)d\nu$$

$$I(\nu) = (2h\nu^{3}/c^{2})\left(\frac{1}{\exp(h\nu/kT_{r})-1}\right)$$

$$R^{r}_{\beta\to\alpha} = 4\pi\left(\frac{\Omega_{\alpha}}{\Omega_{\beta}}e^{U_{\alpha\to\beta}}\right)\int_{0}^{\infty}(\sigma_{\alpha\to\beta}(\nu)/h\nu)((2h\nu^{3}/c^{2})+I(\nu))e^{-h\nu/kT_{e}}d\nu$$

$$U_{\alpha\to\beta} = \frac{\left(E(\beta)-E(\alpha)\right)}{kT_{e}}$$

$$\sigma_{\alpha\to\beta}(\nu) = \frac{\pi e^{2}}{mc}f_{\alpha\to\beta}\phi_{\alpha\to\beta}(\nu)$$

Photopumping

If photon intensity is roughly constant over the line shape then we can approximate it as a delta function

$$\phi_{\alpha\to\beta}(\nu) = \delta(\nu - \nu_0)$$

which leads to the radiative excitation and de-excitation rates being

$$R^r_{\alpha\to\beta} = A_{\beta\to\alpha} n_{ph}$$

$$R^r_{\beta\to\alpha} = A_{\beta\to\alpha}(1 + n_{ph})$$

$$n_{ph} = \frac{1}{e^{h\nu_0 / kT_b} - 1}$$

$$A_{\beta\to\alpha} = \frac{8\pi^2 e^2 \varepsilon_0^2}{h^2 mc^3} \frac{\Omega_\alpha}{\Omega_\beta} f_{\alpha\to\beta}$$

Photoionisation / photorecombination rates

Both rates involve an integral over the photoionisation cross-section and the radiation field

$$R^r_{\alpha\to\beta'} = 4\pi\int_0^\infty (\sigma_{\alpha\to\beta'}(\nu) I(\nu)/h\nu) d\nu$$

$$I(\nu) = (2h\nu^3/c^2)\left(\frac{1}{\exp(h\nu/kT_r)-1}\right)$$

$$R^r_{\beta'\to\alpha} = 4\pi\left(\frac{n^e}{2}\left(\frac{h^2}{2\pi m_e k T_e}\right)^{3/2}\frac{\Omega_\alpha}{\Omega_{\beta'}} e^{U_{\alpha\to\beta'}}\right)\int_0^\infty (\sigma_{\alpha\to\beta'}(\nu)/h\nu)((2h\nu^3/c^2)+I(\nu))e^{-h\nu/kT_e} d\nu$$

$$U_{\alpha\to\beta'} = \frac{\left(E(\beta')-E(\alpha)\right)}{kT_e}$$

Radiative rates - no radiation field

If there is no ambient radiation field only spontaneous de-excitation and radiative recombination remain

$$R^r_{\beta\to\alpha} = A_{\beta\to\alpha}$$

$$R^r_{\beta'\to\alpha} = 4\pi\left(\frac{n^e}{2}\left(\frac{h^2}{2\pi\, m_e k\, T_e}\right)^{3/2}\frac{\Omega_\alpha}{\Omega_{\beta'}}e^{U_{\alpha\to\beta'}}\right)\int_0^\infty(\sigma_{\alpha\to\beta'}(\nu)/h\nu)(2h\nu^3/c^2)e^{-h\nu/kT_e}d\nu$$

No external radiation field – optical depth

But even if no radiation is incident on the plasma from outside, internally generated radiation from transitions can influence the populations.

This introduces the photon escape probability $g(\tau_0)$

$$R^r_{\alpha\to\beta} = 0$$

$$R^r_{\beta\to\alpha} = A_{\beta\to\alpha}\, g(\tau_0)$$

For a Doppler lineshape this is given by

$$g(\tau_0) = \frac{1}{\tau_0}\int_{-\infty}^{\infty}(1-\exp(-\tau_0 e^{-x^2}))dx$$

$$\phi(\nu) = \frac{1}{\sqrt{\pi}\Delta\nu_D}e^{-x^2}$$

$$x = (\nu-\nu_0)/\Delta\nu_D$$

$$\Delta\nu_D = \frac{(2kT_i)^{1/2}}{m}\frac{\nu_0}{c}$$

Optical depth

$$\tau_0 = \frac{\pi e^2}{mc} f_{\alpha\to\beta}\phi(\nu_0)(n_\alpha - \frac{\Omega_\alpha}{\Omega_\beta}n_\beta)y$$

Cauchy (Dirac-Fuchs) mean chord theorem

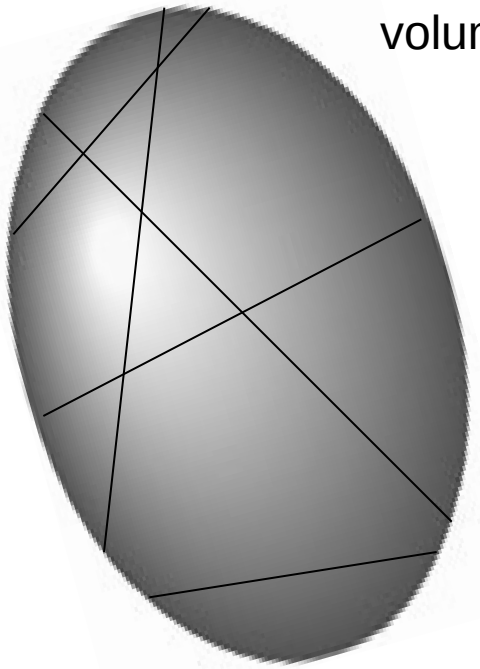

For any convex shape, the mean chord length is given by the Dirac-Fuchs theroem as ***y = 4V/A***

For a slab geometry, *the mean chord length* $y = 4V/A = 2z_0$

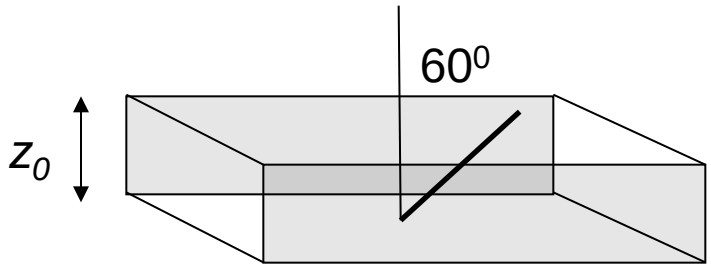

Dirac P A M, Technical Report MS-D-5, part I, Public Records Office, Kew (1943).
Dirac PAM, Fuchs K, Peierls R and Preston P, Technical Report MS-D-5, part II, Public Records Office, Kew (1943).

Level of detail describing atomic states

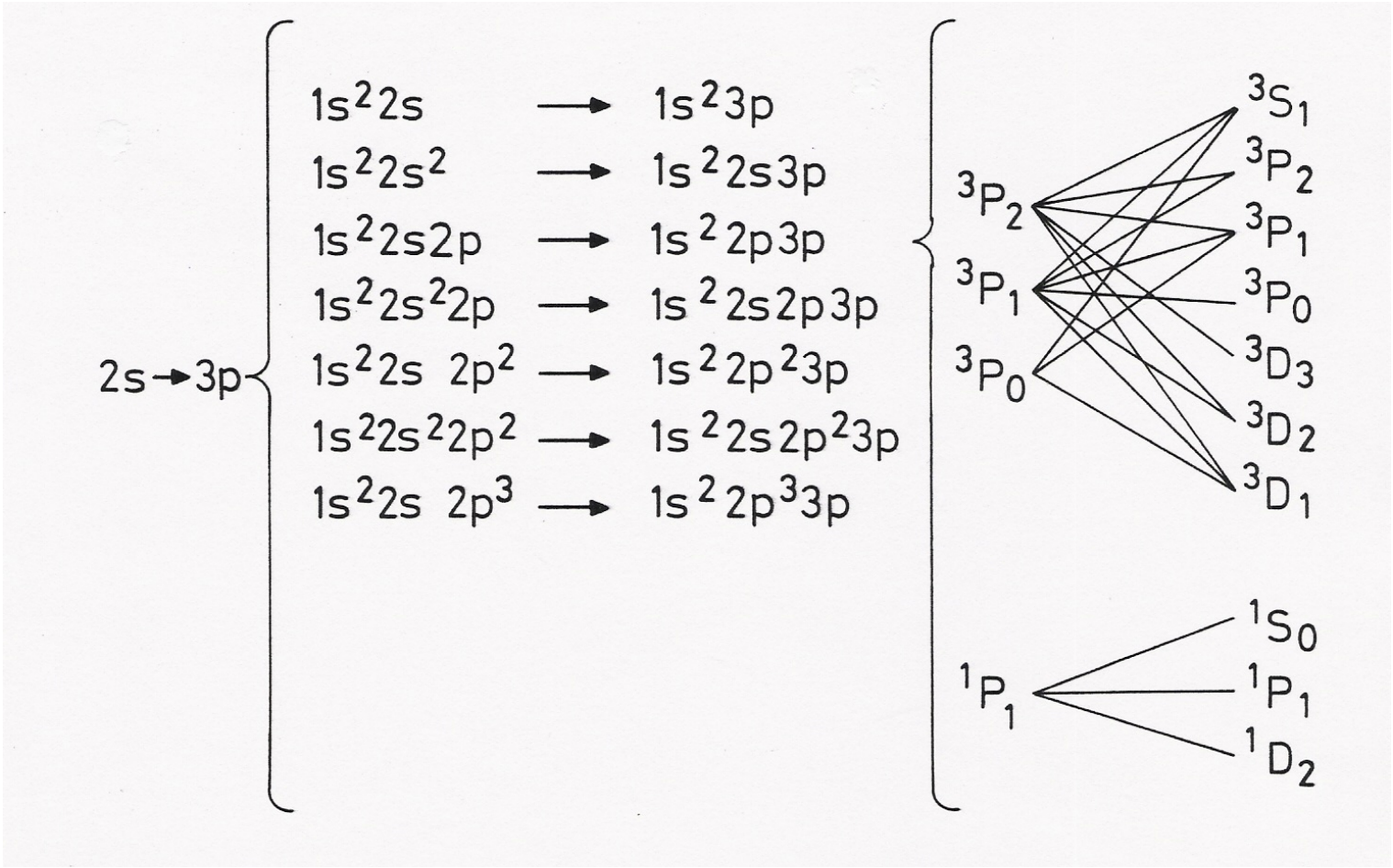

Average-atom

Detailed Configuration Accounting DCA

Detailed Term Accounting DTA

Average-atom model

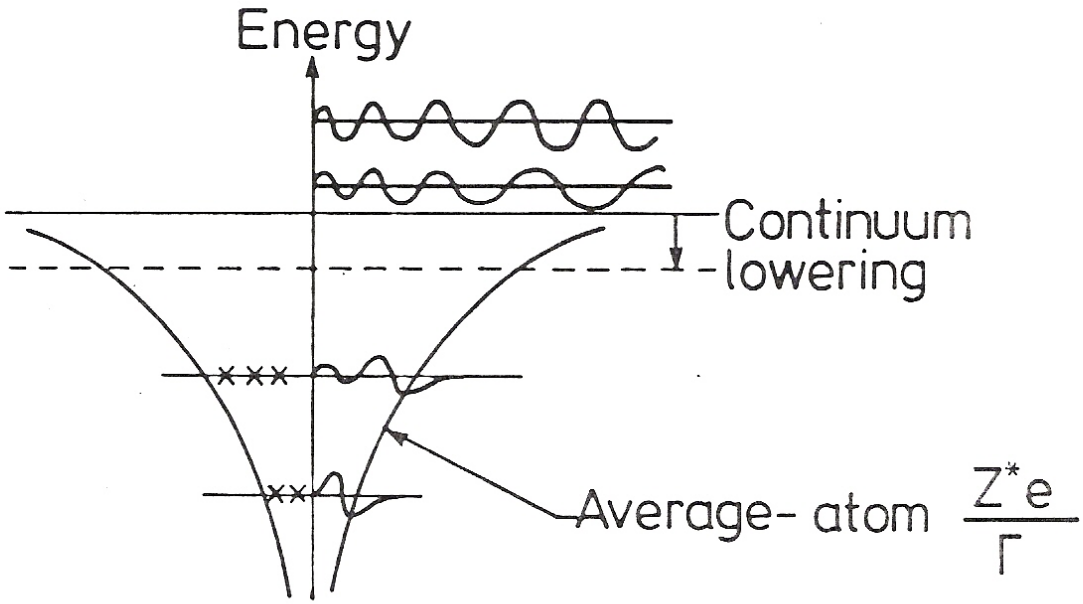

Collisional and radiative rates

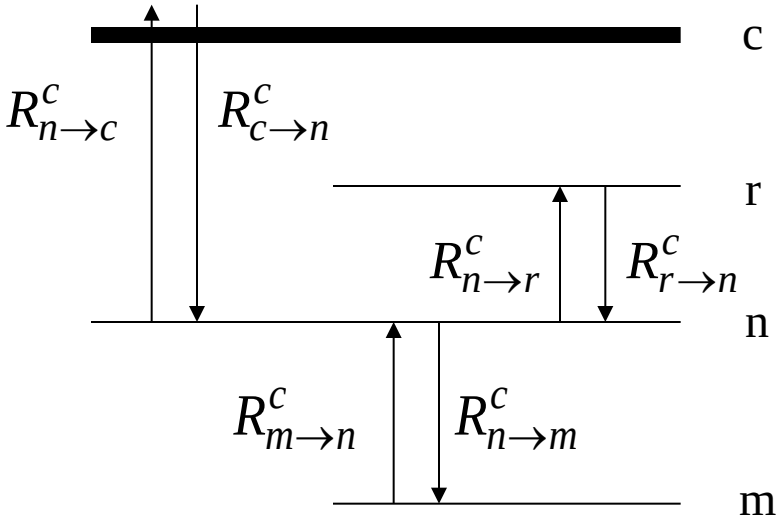

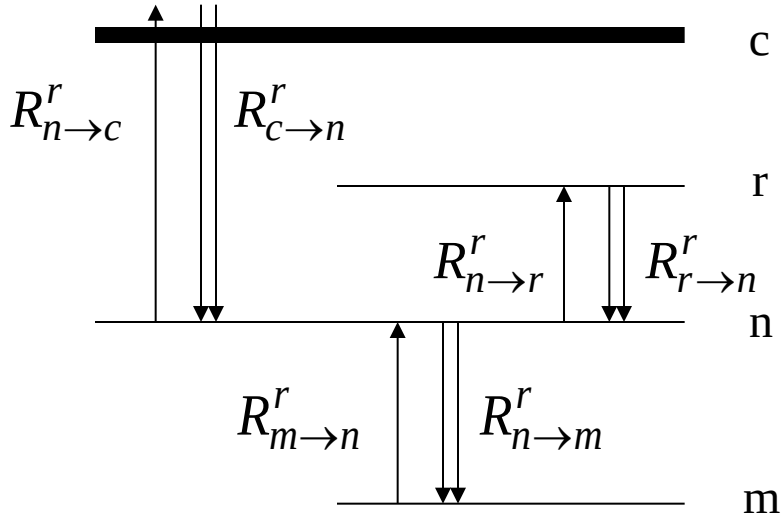

NIMP – equations and solutions

sum of radiative and collisional rates from shell m to n

$$\frac{dP_n}{dt} = - - - + P_m \left(1 - \frac{P_n}{\omega_n}\right)(R^c_{m\to n} + R^r_{m\to n}) + - - -$$

number of electrons in shell m

probability of a hole in shell n

screened-hydrogenic excitation and ionisation energies, collisional and radiative rates used

$$\frac{dP_1}{dt} = f_1(P_1, ..., P_{n\max}, R)$$

$$\vdots$$

$$\frac{dP_{n\max}}{dt} = f_{n\max}(P_1, ..., P_{n\max}, R)$$

solved for

$$P_1, ..., P_{n\max}$$

Reconstruction of individual level populations from the average shell populations

From the average populations $(P_1,\ldots,P_{nmax})$ the fraction of ions in a real configuration $\alpha(n_1,\ldots,n_{nmax})$ can be calculated assuming that the orbitals are not statistically correlated

$$P(\alpha) = \prod_i \frac{\omega_i!}{(\omega_i - n_i)!n_i!}\left(\frac{P_i}{\omega_i}\right)^{n_i}\left(1-\frac{P_i}{\omega_i}\right)^{\omega_i - n_i}$$

The fraction of ions in level a, degeneracy $2J_a+1$, which is derived from the configuration α, is then

$$P(a) = \left[(2J_a+1)/\left(\frac{\omega_i!}{(\omega_i - n_i)!n_i!}\right)\right]P(\alpha)$$

Photoionisation cross sections

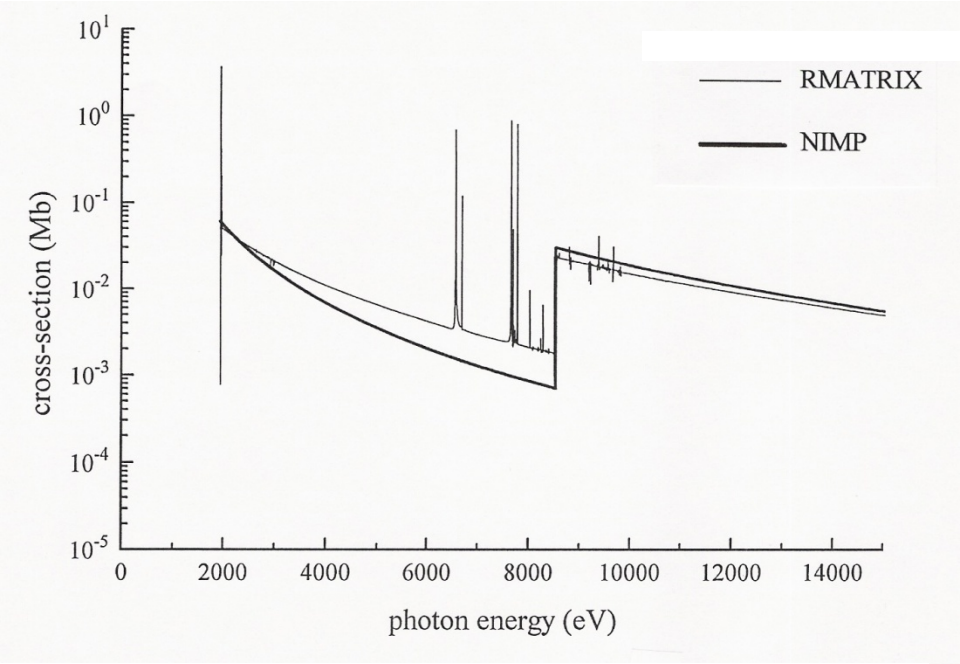

FeXXIII ($1s^2 2s^2$)

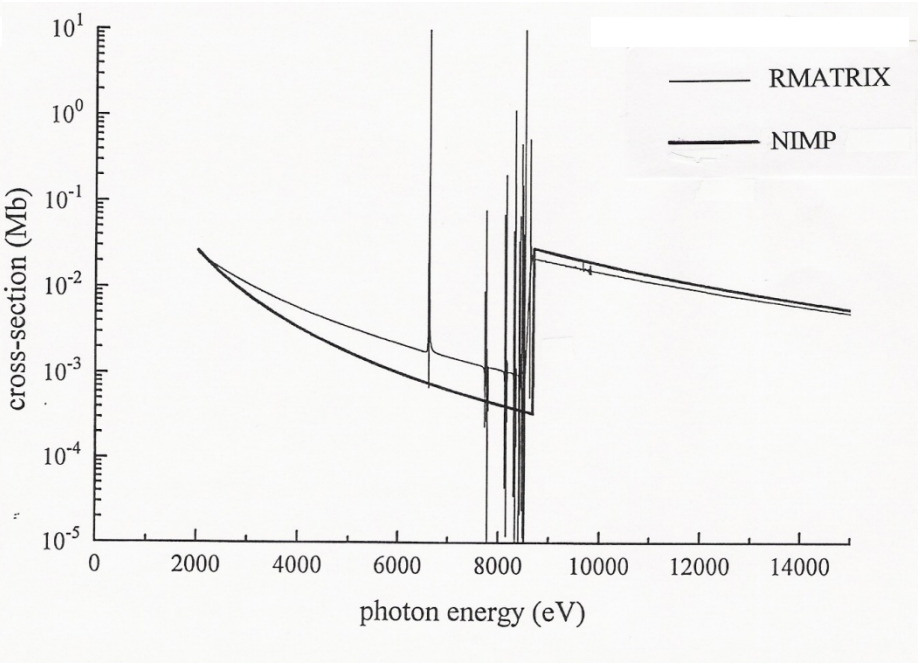

FeXXIV ($1s^2 2s$)

Dielectronic recombination / autoionisation rates

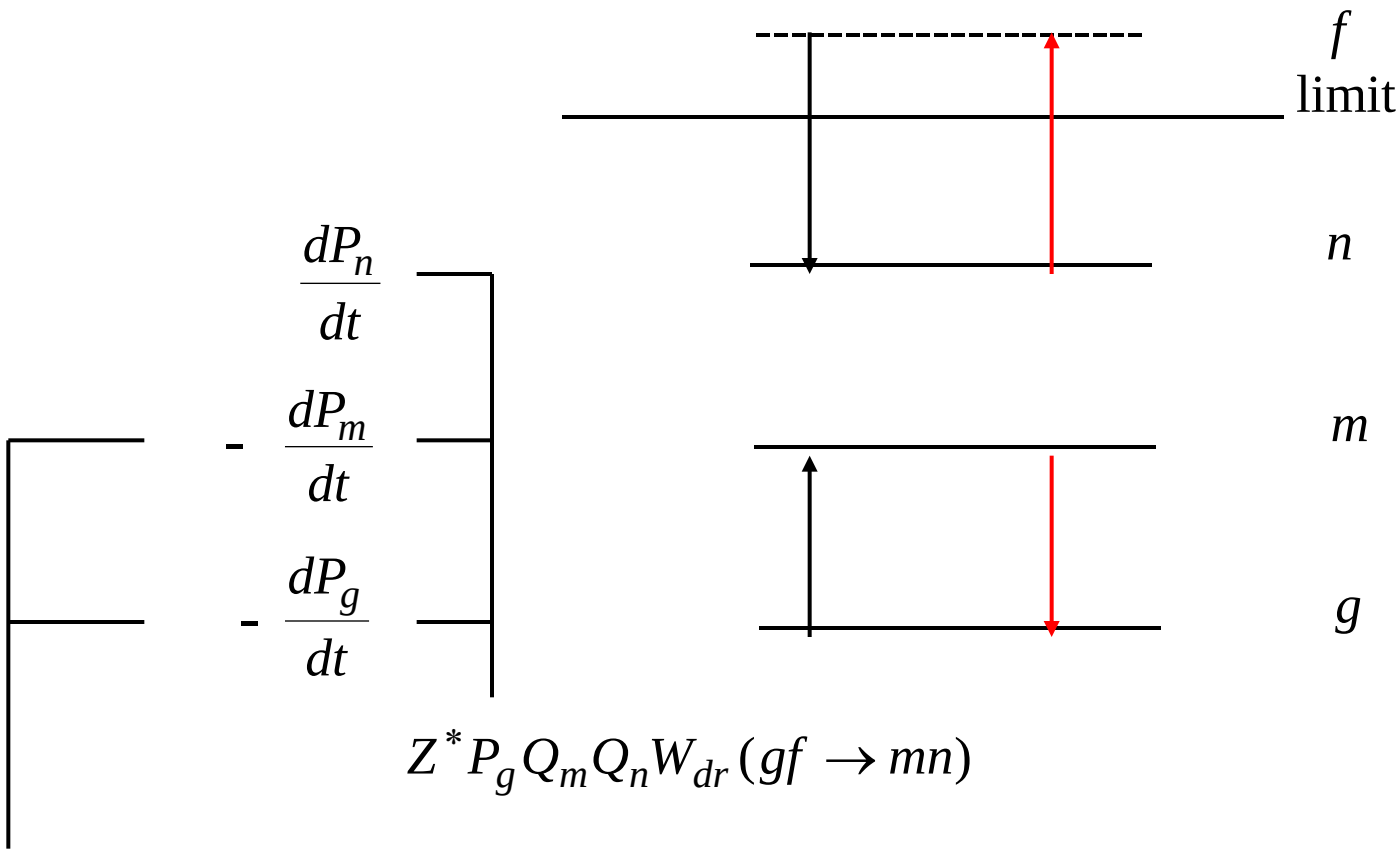

$$Z^* P_g Q_m Q_n W_{dr}(gf \rightarrow mn)$$

$$P_g Q_m R_{g\rightarrow m} \quad \text{with} \quad R_{g\rightarrow m} = Z^* Q_n W_{dr}(gf \rightarrow mn)$$

detailed balance $$Z^{*0} P_g^0 Q_m^0 Q_n^0 W_{dr}(gf \rightarrow mn) = P_n^0 P_m^0 Q_g^0 W_a(mn \rightarrow gf)$$

Albritton and Wilson, Phys Rev Letts, **83**, 1594 (1999); JQSRT, **65**, 1 (2000)

Comparison of NIMP and detailed (DCA) models with / without DR

Se $n_e=5x10^{20}cm^{-3}$, $T_e=1000eV$

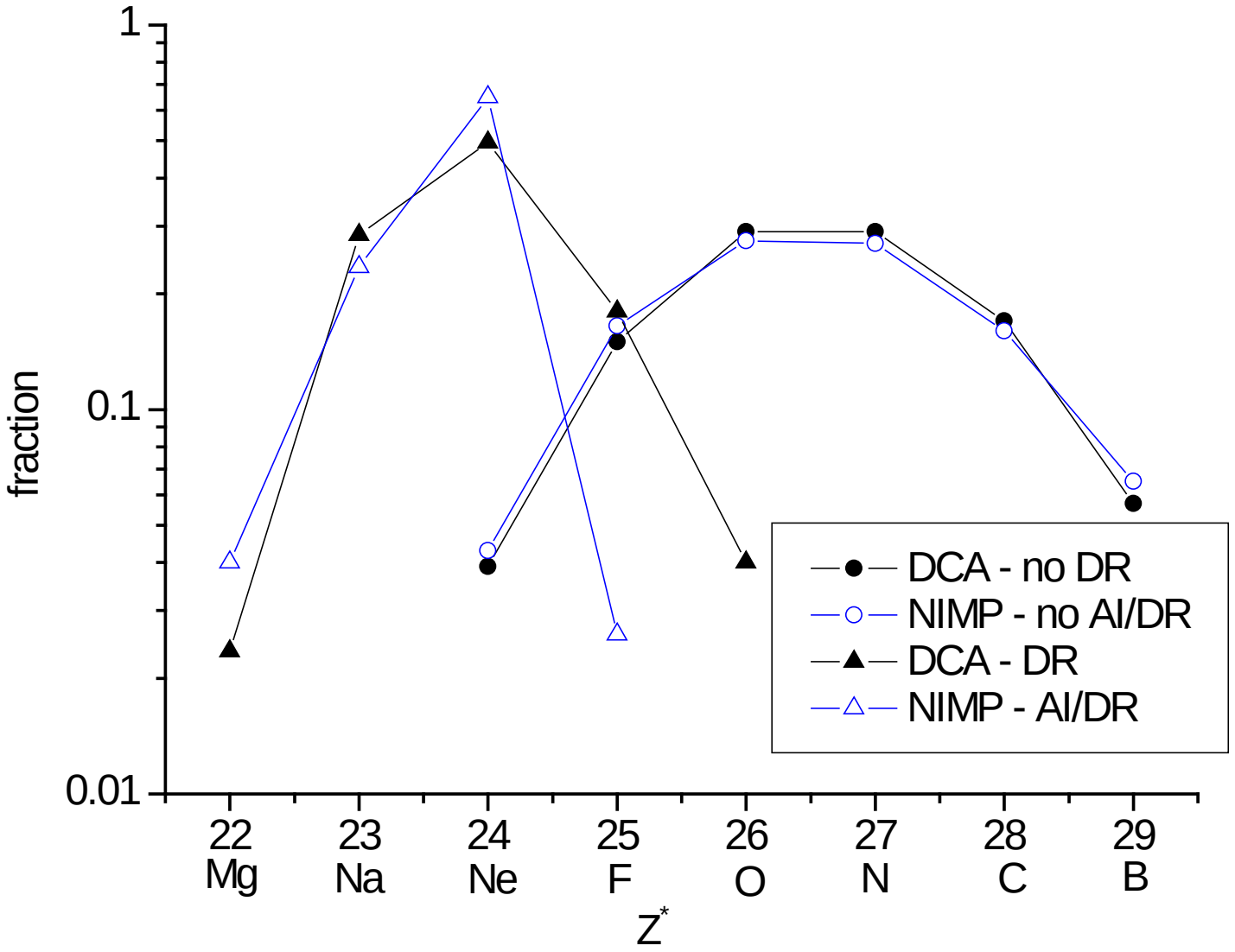

Lee, JQSRT, **38**, 131 (1987)

Comparison between theory and experiment

No or small radiation field

Non-LTE ionisation distribution measurement

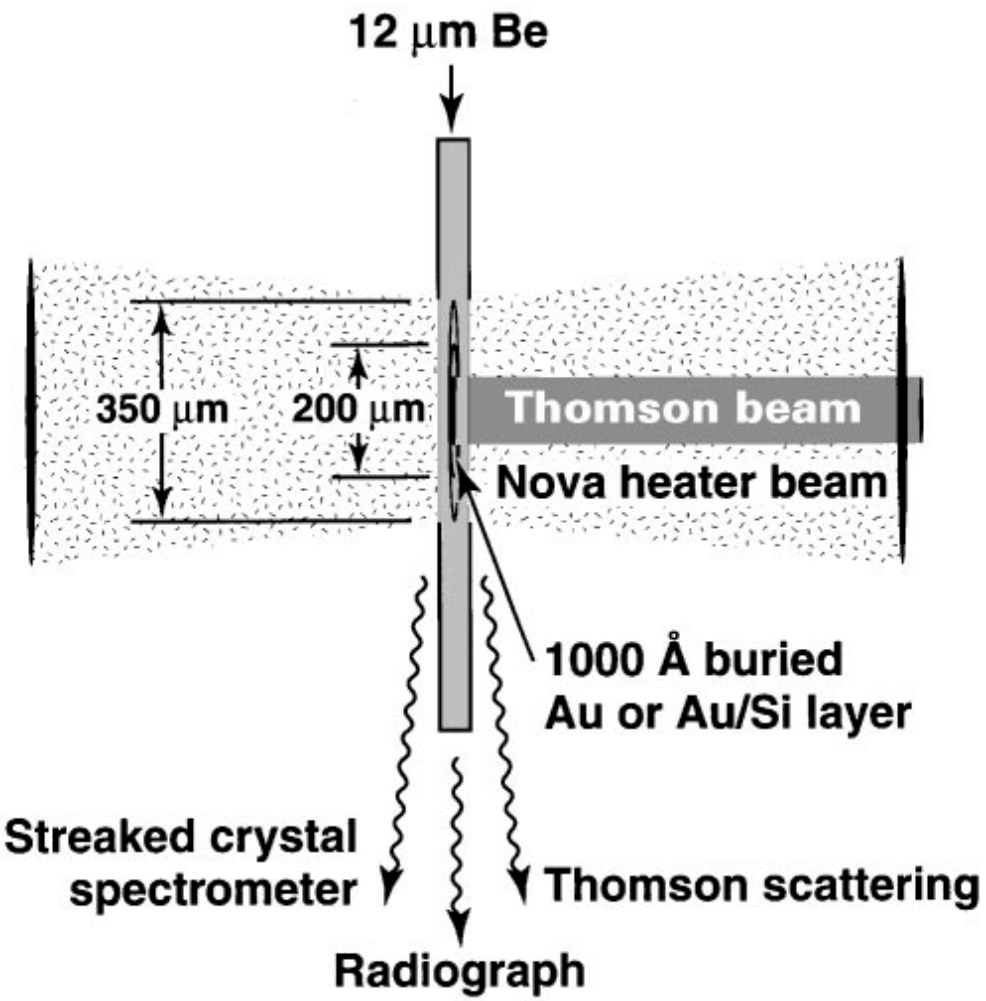

Conditions in the gold plasma were characterised by Thompson scattering, radiography and X-ray spectroscopy.

Foord, Glenzer, Thoe, Wong, Fournier, Wilson, Springer, Phys Rev Letts, **85**, 992 (2000).
Foord, Glenzer, Thoe, Wong, Fournier, Albritton, Wilson, Springer, JQSRT, **65**, 231 (2000).

Charge state distributions for Au
$n_e=6x10^{20}cm^{-3}$, $T_e=2200eV$

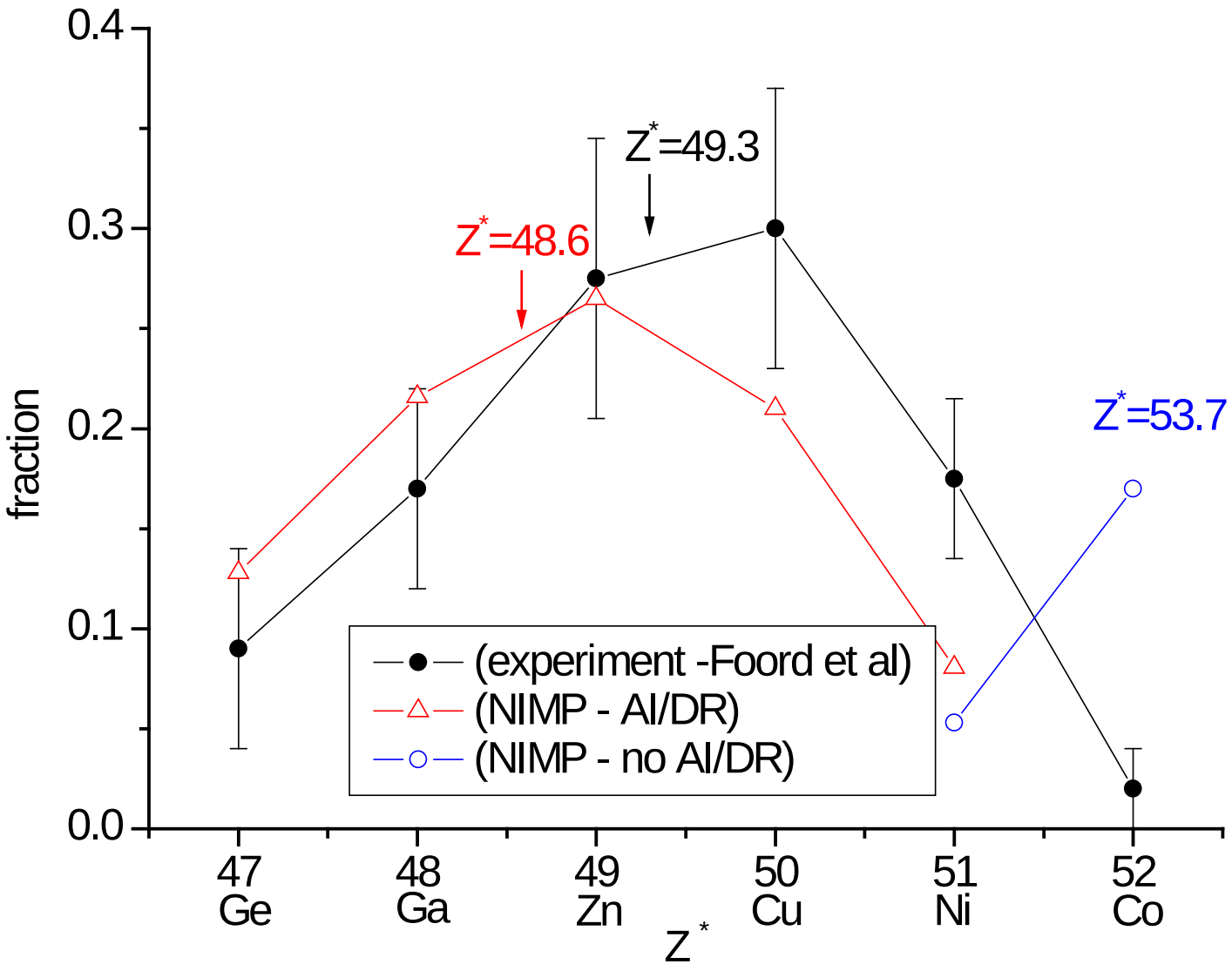

Charge state distributions for Au
$n_e=1.4x10^{21}cm^{-3}$, $T_e=2600eV$

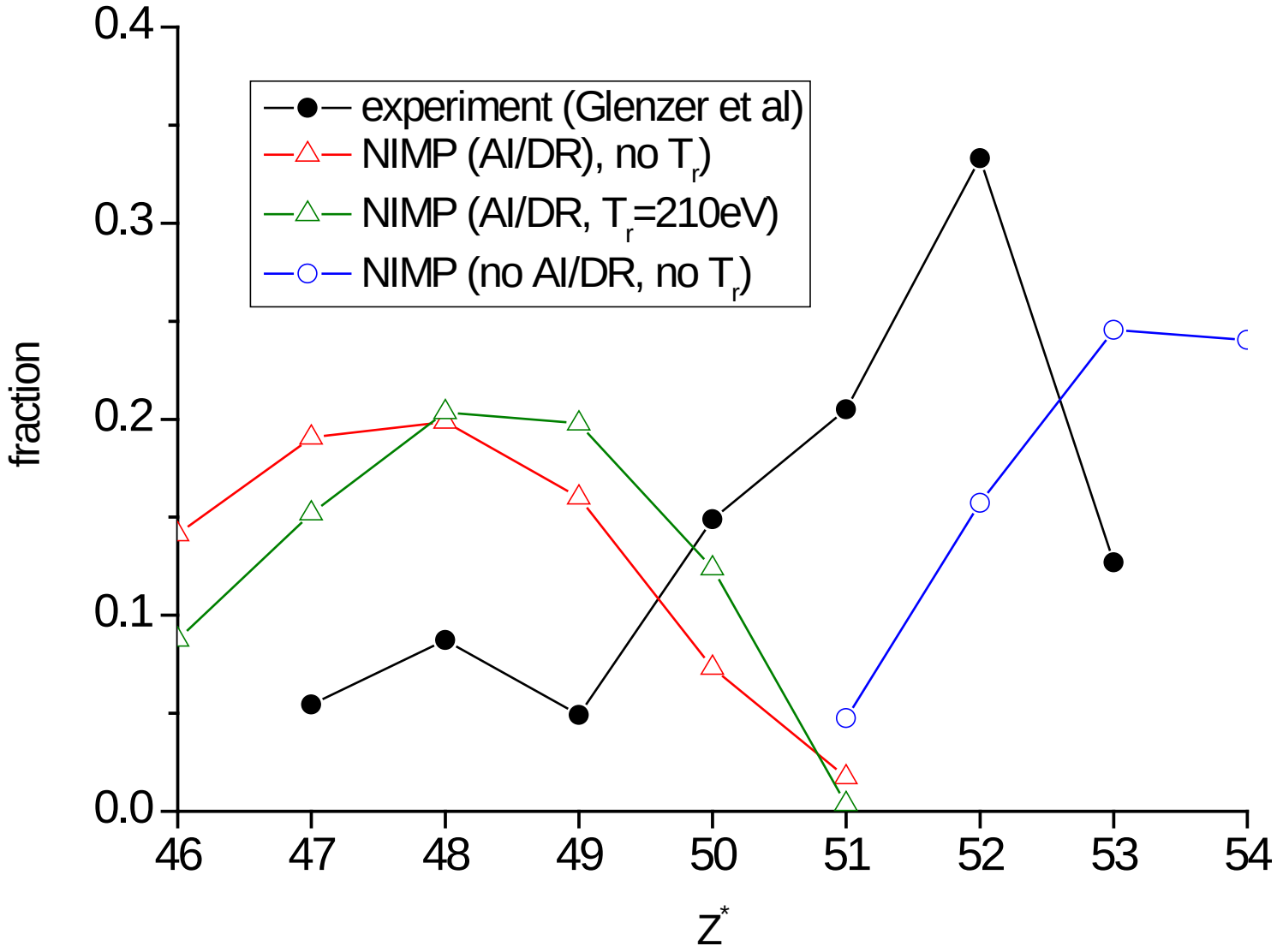

Glenzer, Fournier, Wilson, Lee and Suter Phys Rev Letts, **65**, 045002 (2001).

Charge state distributions for Xe
$n_e=1.3x10^{20}cm^{-3}$, $T_e=415eV$

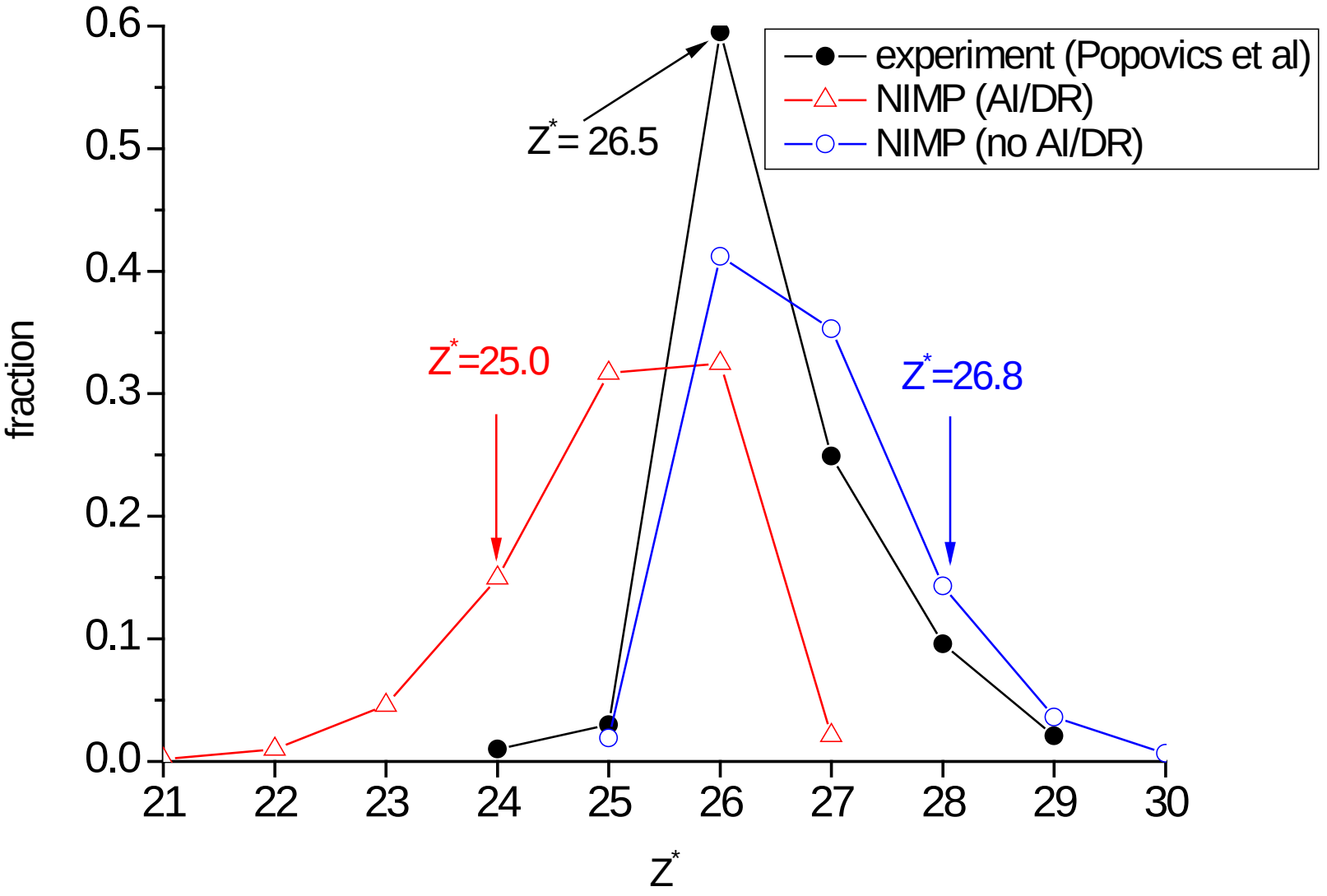

Chenais-Popovics, Malka, Gauthier, Gary, Peyrusse, Rabec-Le Gloahec, Matsushima, Bauche-Arnoult, Bachelier and Bauche Phys Rev E, **65**, 046418 (2002).

Charge state distributions for Au
$n_e=10^{12}cm^{-3}$, $T_e=2500eV$

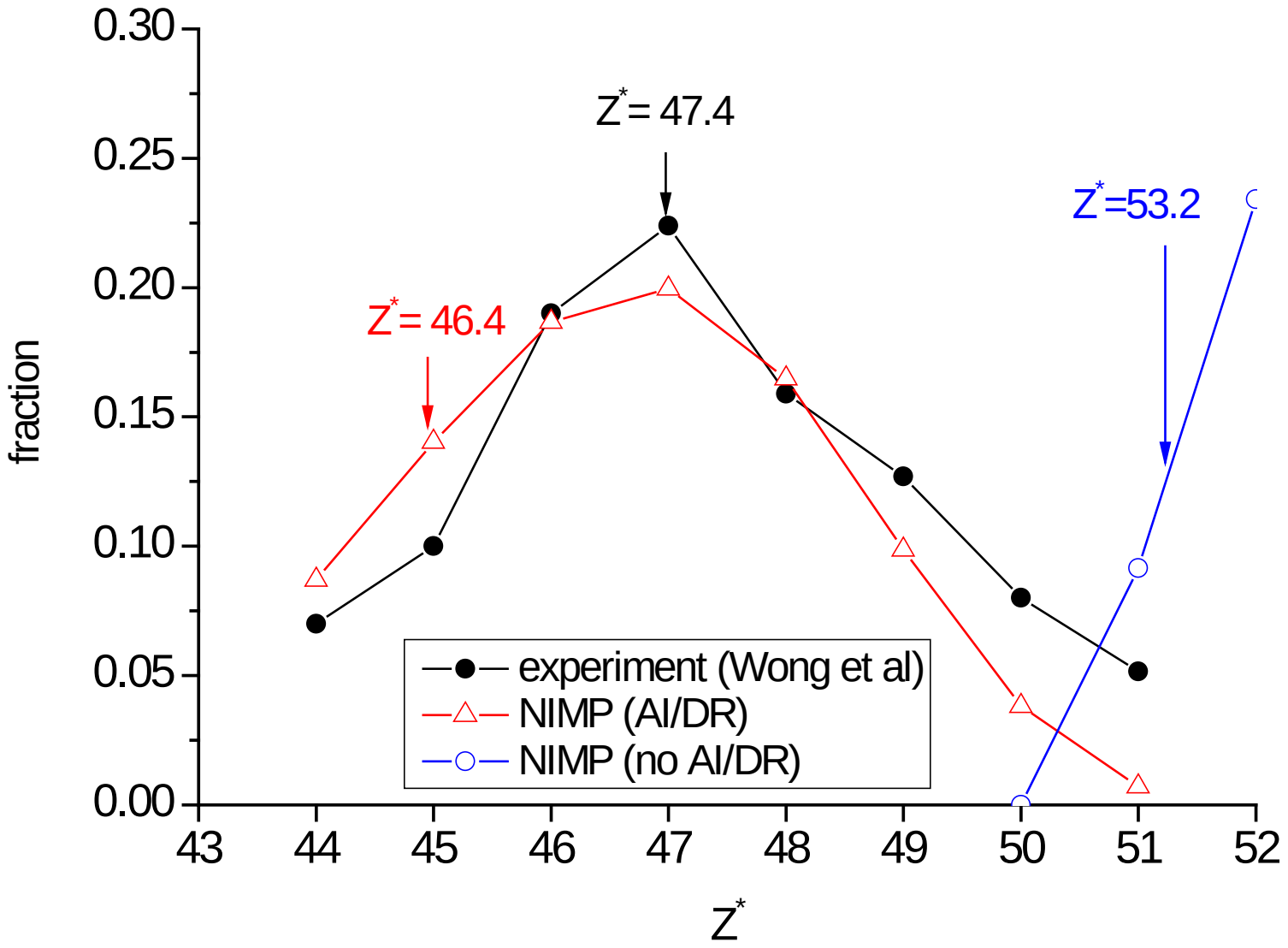

Wong, May, Beiersdorfer, Fournier, Wilson, Brown, Springer, Neill and Harris, Phys Rev Letts, **90**, 235001 (2003).

Ionisation in Au, $n_e=10^{21}cm^{-3}$ with and without a radiation field

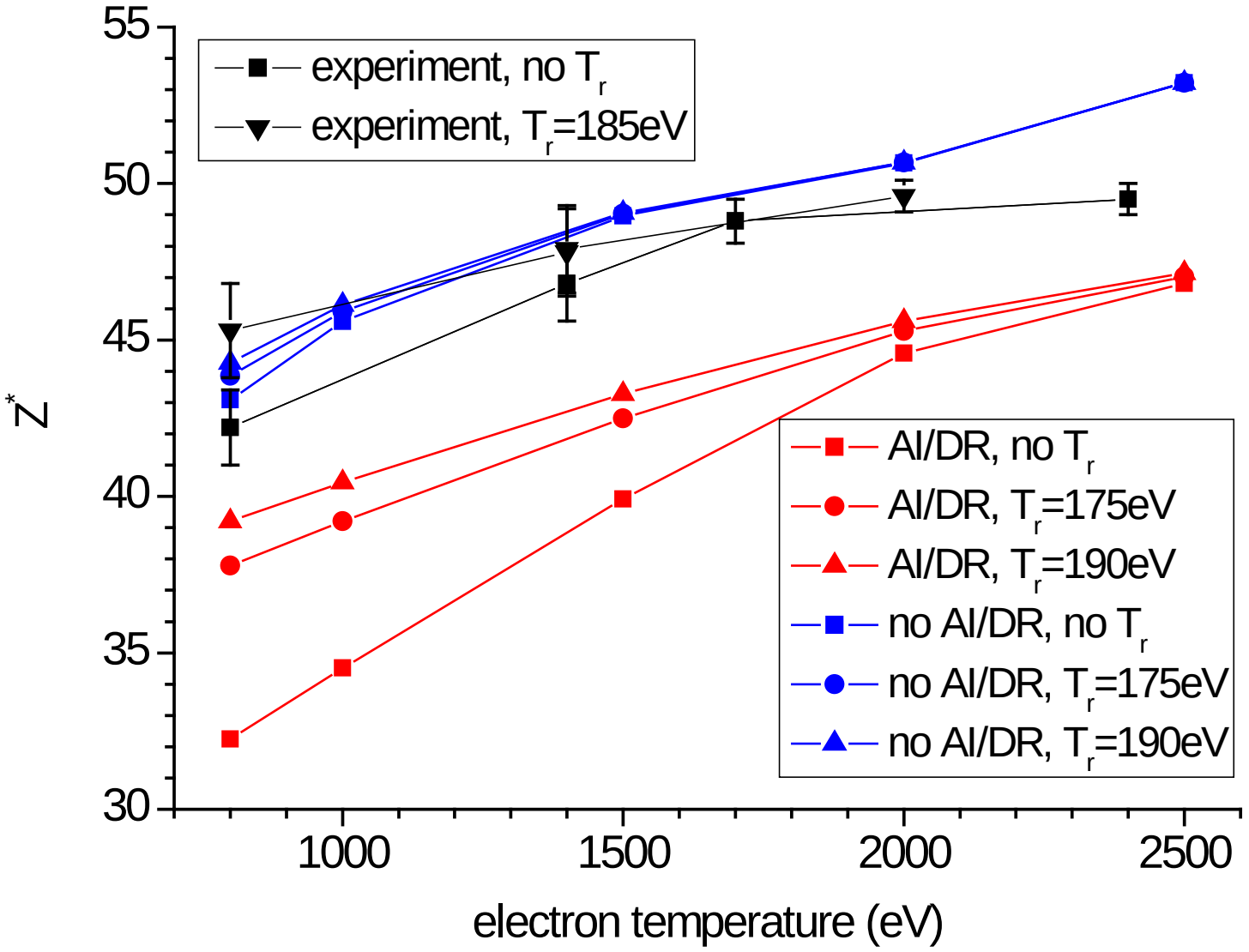

Heeter, Hansen, Fournier, Foord, Froula, Mackinnon, May, Schneider and Young Phys Rev Letts, **99**, 195001 (2007).

Comparison between theory and experiment

Broad-band radiation field

Photoionised plasmas

Accretion-powered objects

Photoionised plasmas (radiation-dominated plasmas) scale with the ionisation parameter $\xi=4\pi F/n_e$

Tarter, Tucker and Salpeter, ApJ, **156**, 943,(1969)
Tarter and Salpeter, ApJ, **156**, 953 (1969)

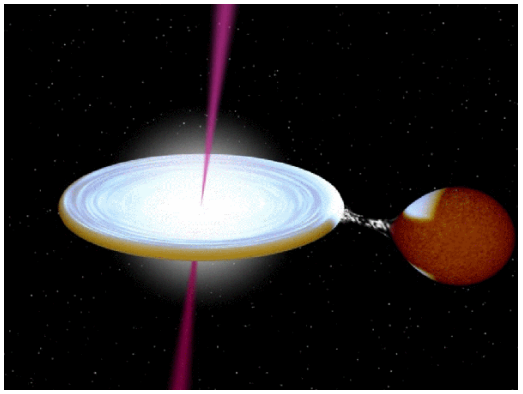

EXO 0748-676

Low mass X-ray binary

ξ=30 ergcms^{-1}

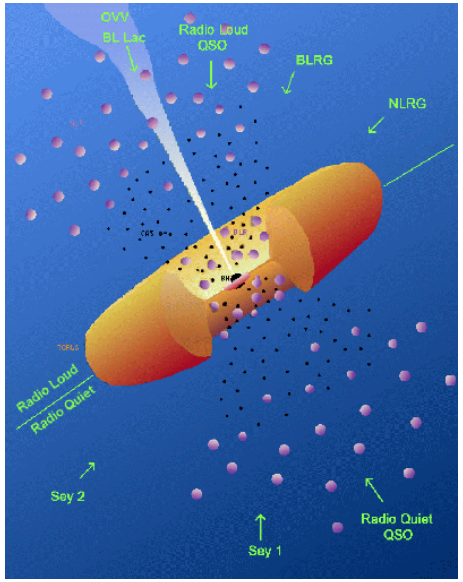

NGC 4593

Seyfert galaxy

ξ=300 ergcms^{-1}

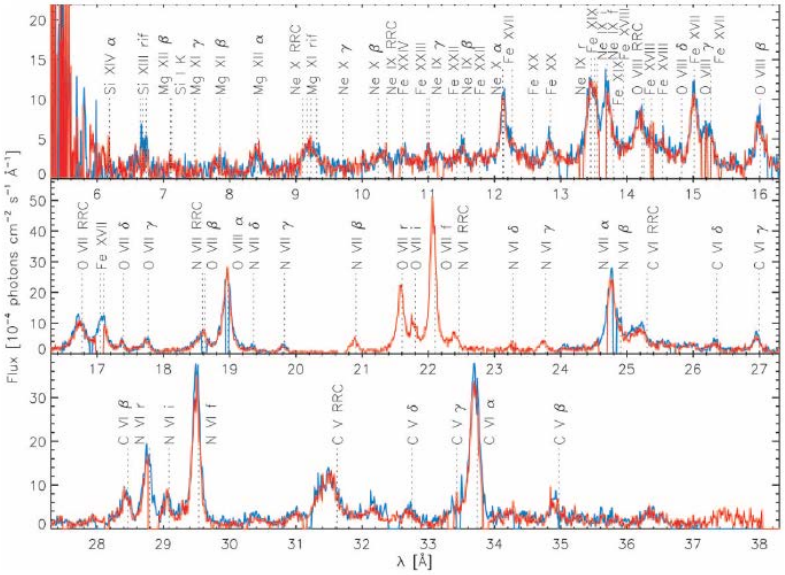

Spectral interpretation needs reliable models

Ionisation / recombination rates

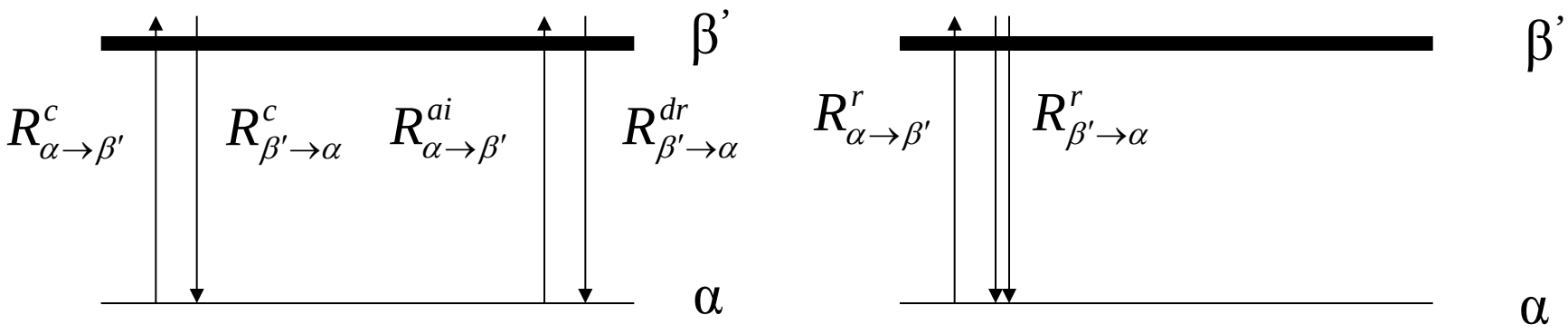

Ionisation / recombination rates

$R^{c}_{\alpha\rightarrow\beta'}$ Electron collisional ionisation (~n_e)

$R^{c}_{\beta'\rightarrow\alpha}$ Three-body recombination (~n_e^2)

$R^{ai}_{\alpha\rightarrow\beta'}$ Autoionisation

$R^{dr}_{\beta'\rightarrow\alpha}$ Dielectronic recombination (~n_e)

$R^{r}_{\alpha\rightarrow\beta'}$ Photoionisation – stimulated absorption

$R^{r}_{\beta'\rightarrow\alpha}$ Photorecombination (~n_e) – spontaneous and stimulated absorption

Ionisation / recombination rates

In the limit of high radiation field and low electron density

$R^{c}_{\alpha\to\beta'}$ Electron collisional ionisation (~n_e)

$R^{c}_{\beta'\to\alpha}$ Three-body recombination (~n_e^2)

$R^{ai}_{\alpha\to\beta'}$ Autoionisation

$R^{dr}_{\beta'\to\alpha}$ Dielectronic recombination (~n_e)

$R^{r}_{\alpha\to\beta'}$ Photoionisation – stimulated absorption

$R^{r}_{\beta'\to\alpha}$ Photorecombination (~n_e) – spontaneous and stimulated absorption

Photoionised plamsas

$$n_\alpha R^r_{\alpha\to\beta'} = n_{\beta'} n_e \alpha_{\beta'\to\alpha}(T_e)$$

ignoring stimulated radiative recombination

$$\alpha_{\beta'\to\alpha}(T_e) = R^{dr}_{\beta'\to\alpha} + R^r_{\beta'\to\alpha}$$

$$\frac{n_{\beta'}}{n_\alpha} = 4\pi \int_0^\infty (\sigma_{\alpha\to\beta'}(\nu) I(\nu)/h\nu) d\nu \Big/ n_e \alpha_{\alpha\to\beta'}(T_e)$$

take out shape function $p(\nu)$ from the flux F

$$\frac{n_{\beta'}}{n_\alpha} = \frac{4\pi F}{n_e} \int_0^\infty (\sigma_{\alpha\to\beta'}(\nu) p(\nu)/h\nu) d\nu \Big/ \alpha_{\alpha\to\beta'}(T_e)$$

$$\xi = \frac{4\pi F}{n_e}$$

Tarter, Tucker and Salpeter, ApJ, **156**, 943,(1969)
Tarter and Salpeter, ApJ, **156**, 953 (1969)

Experiment on Z-pinch at Sandia generates $\xi=20 erg cm s^{-1}$

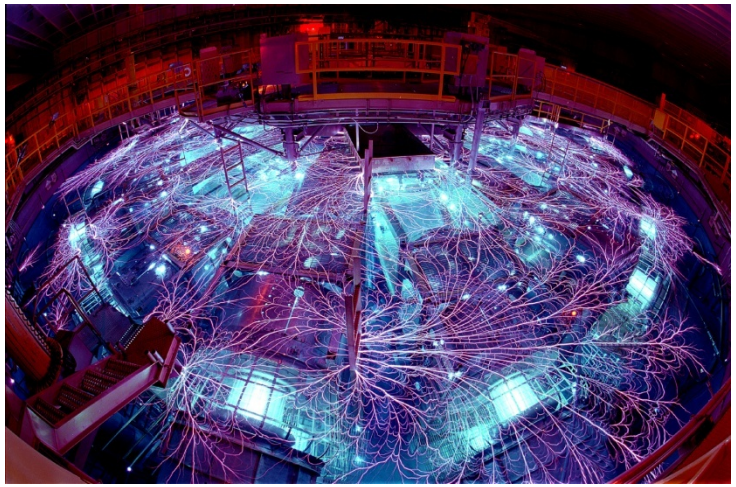

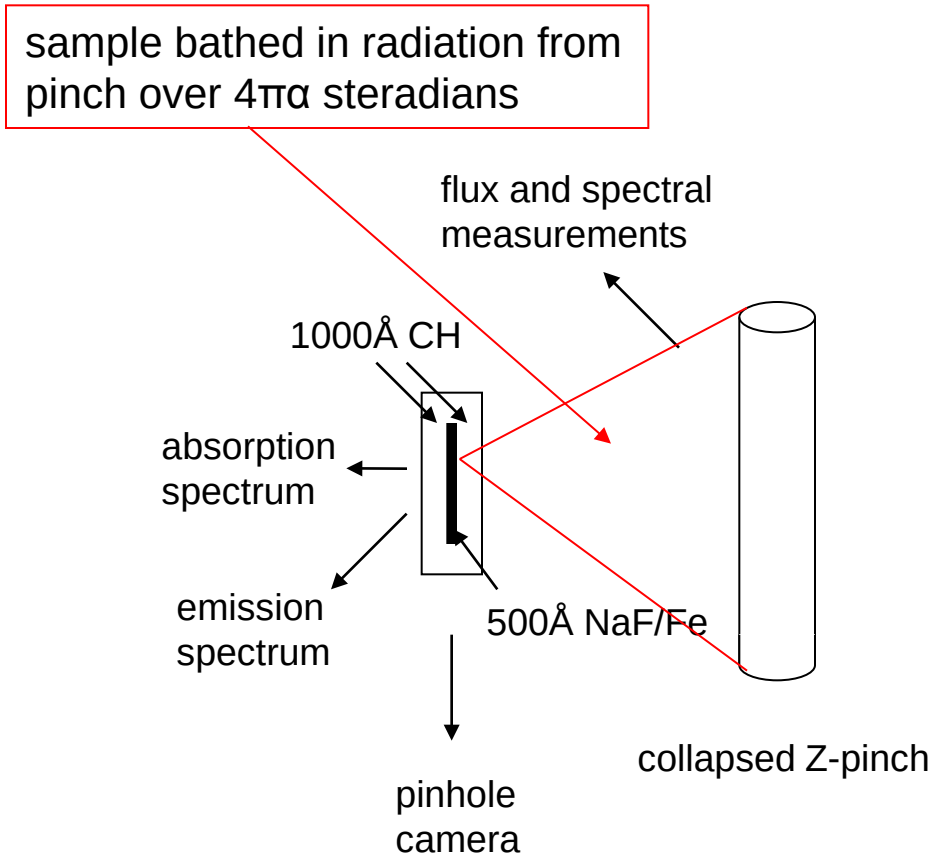

Foord, Heeter, van Hoof, Thoe, Bailey, Cuneo, Chung, Liedahl, Fournier, Chandler, Jonauskas, Kisielius, Mix, Ramsbottom, Springer, Keenan, Rose and Goldstein, Phys Rev Letts, **93**, 055002 (2004)

F photoionised plasma ionisation distribution
$n_e=2x10^{19}$, $T_e=150eV$, $T_r=165eV$ ($\alpha=0.01$), $\xi=20ergcms^{-1}$

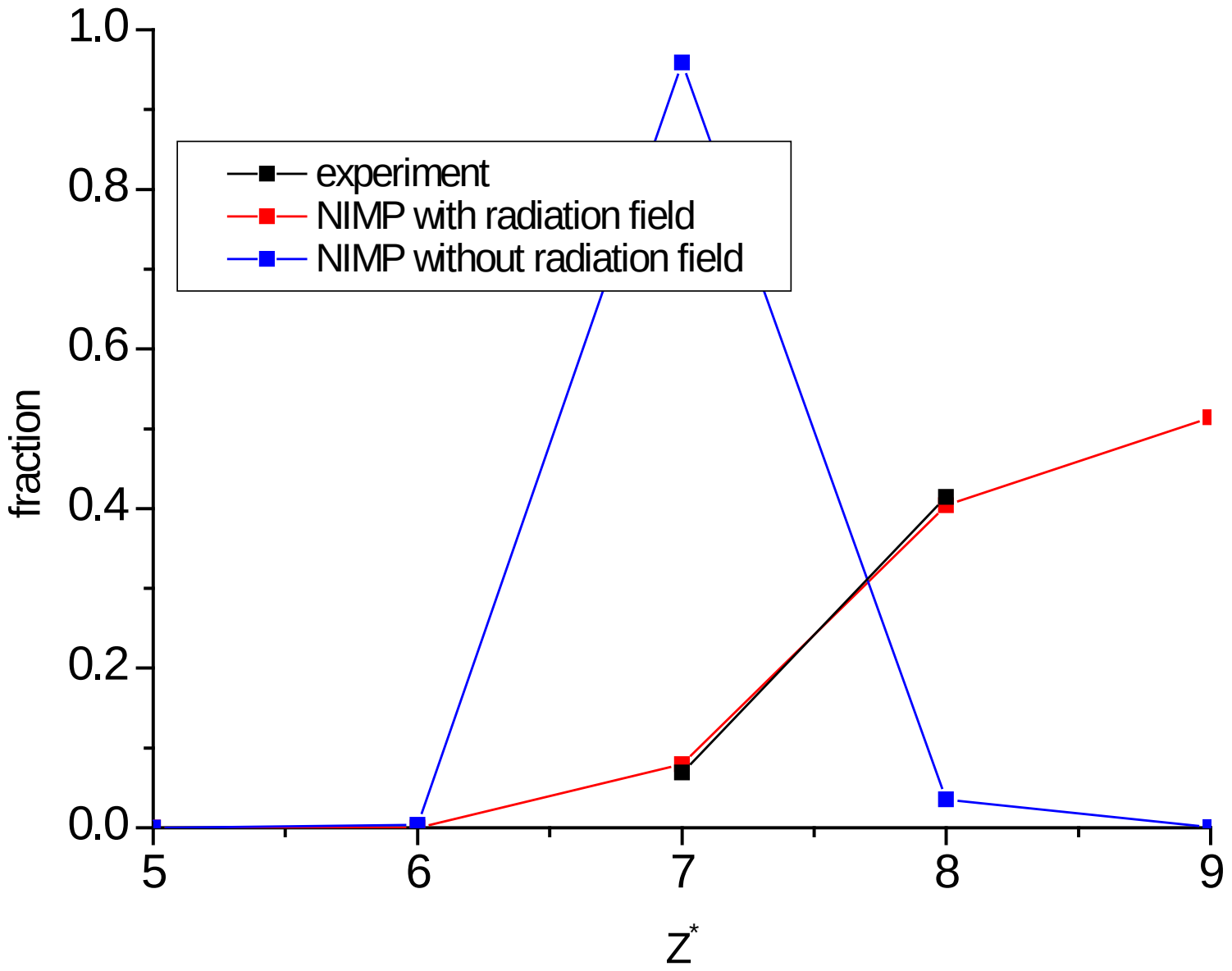

Rose, vanHoof, Jonauskas, Keenan, Kisielius, Ramsbottom, Foord, Heeter and Springer, J Phys B, **37**, L337 (2004)

Na photoionised plasma ionisation distribution
$n_e=2x10^{19}$, $T_e=150eV$, $T_r=165eV$ ($\alpha=0.01$), $\xi=20ergcms^{-1}$

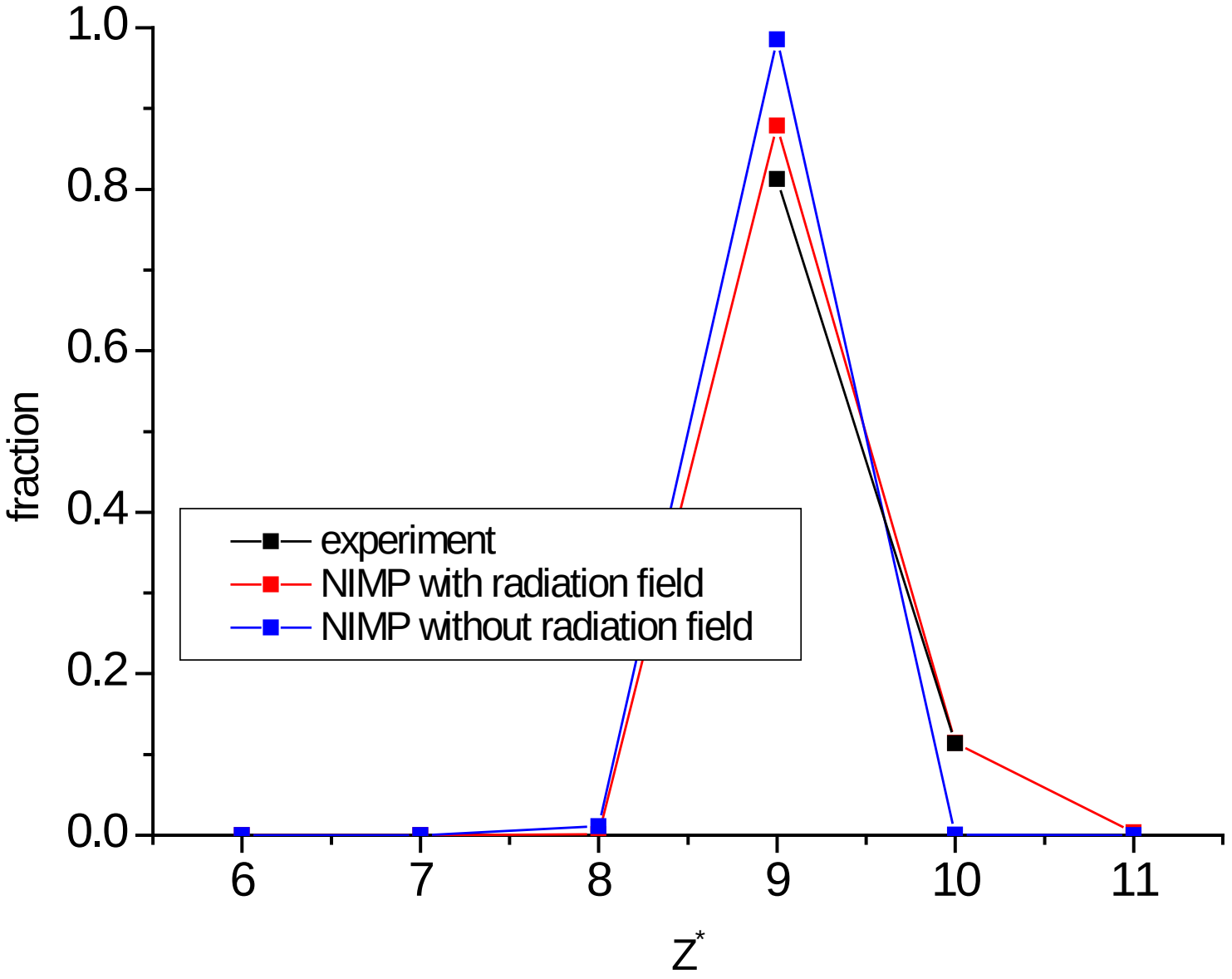

Rose, vanHoof, Jonauskas, Keenan, Kisielius, Ramsbottom, Foord, Heeter and Springer, J Phys B, **37**, L337 (2004)

Fe photoionised plasma ionisation distribution
$n_e=2x10^{19}$, $T_e=150eV$, $T_r=165eV$ ($\alpha=0.01$), $\xi=20ergcms^{-1}$

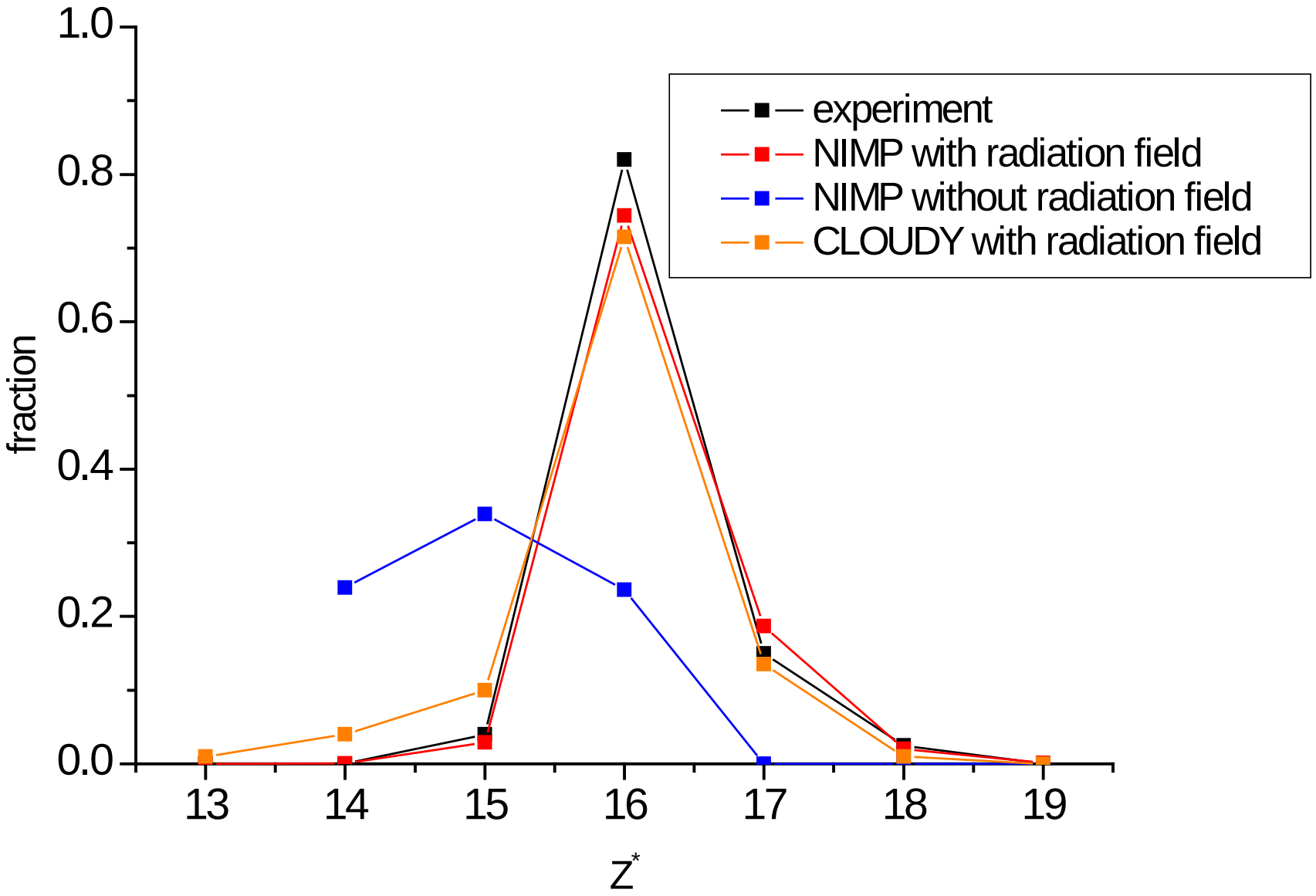

Rose, vanHoof, Jonauskas, Keenan, Kisielius, Ramsbottom, Foord, Heeter and Springer, J Phys B, **37**, L337 (2004)

Z^*(Br) in $C_{500}H_{470}Br_{27}$ 0.001gcm^{-3}

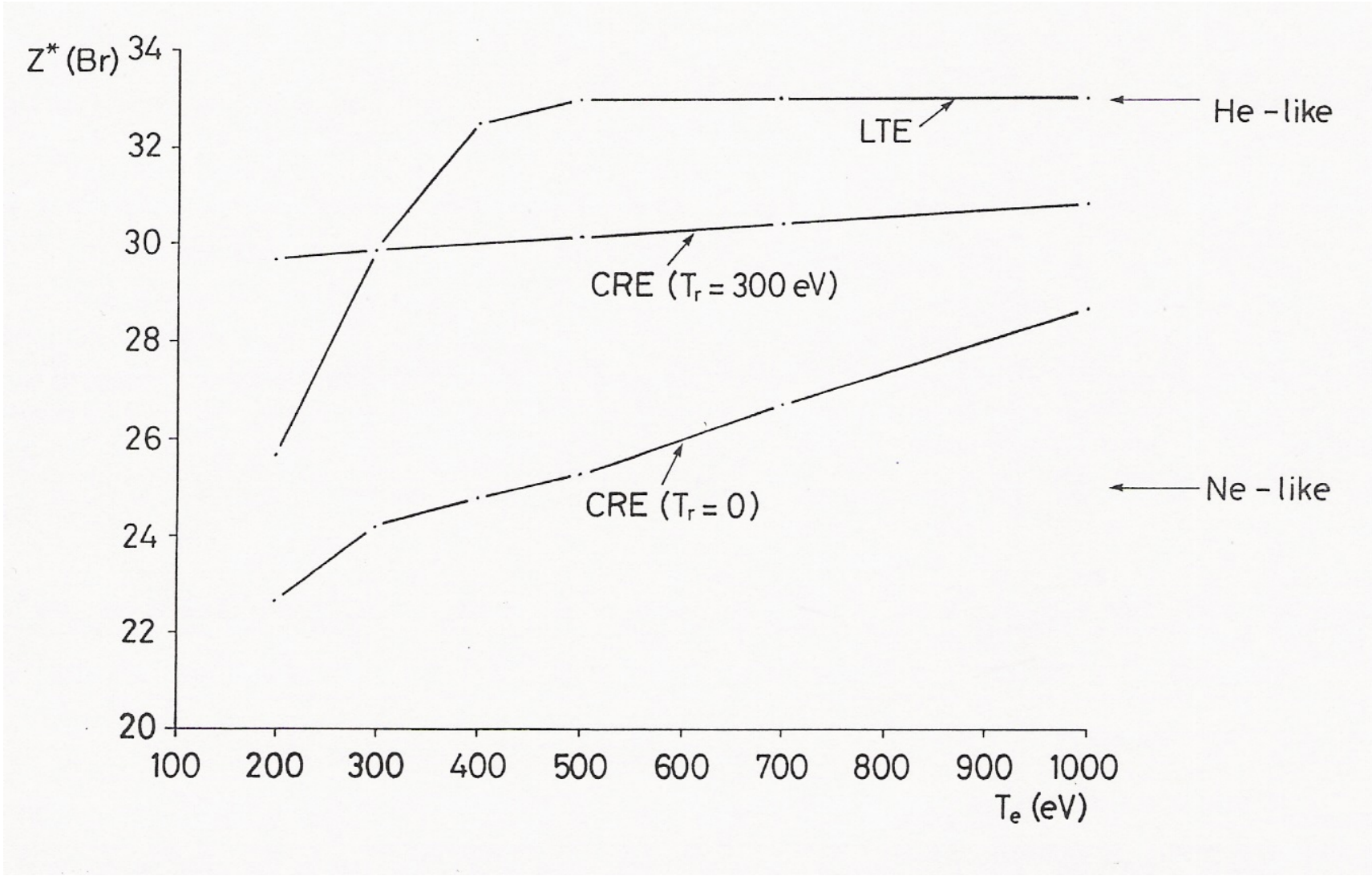

Rose, JQSRT (1995)

Z^*(Br) in $C_{500}H_{470}Br_{27}$ 0.1gcm^{-3}

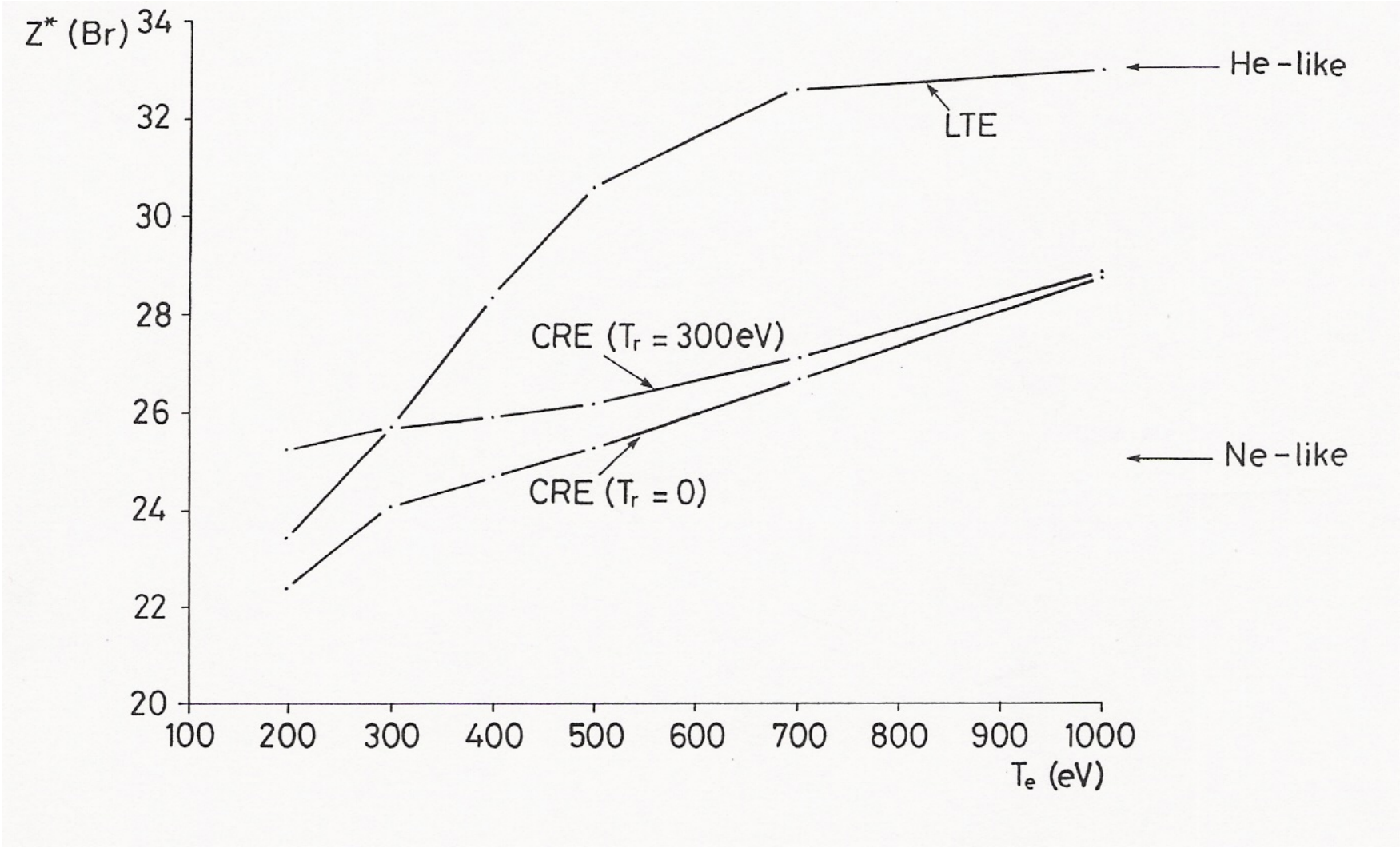

$C_{500}H_{470}Br_{27}$ opacity 0.001gcm^{-3}

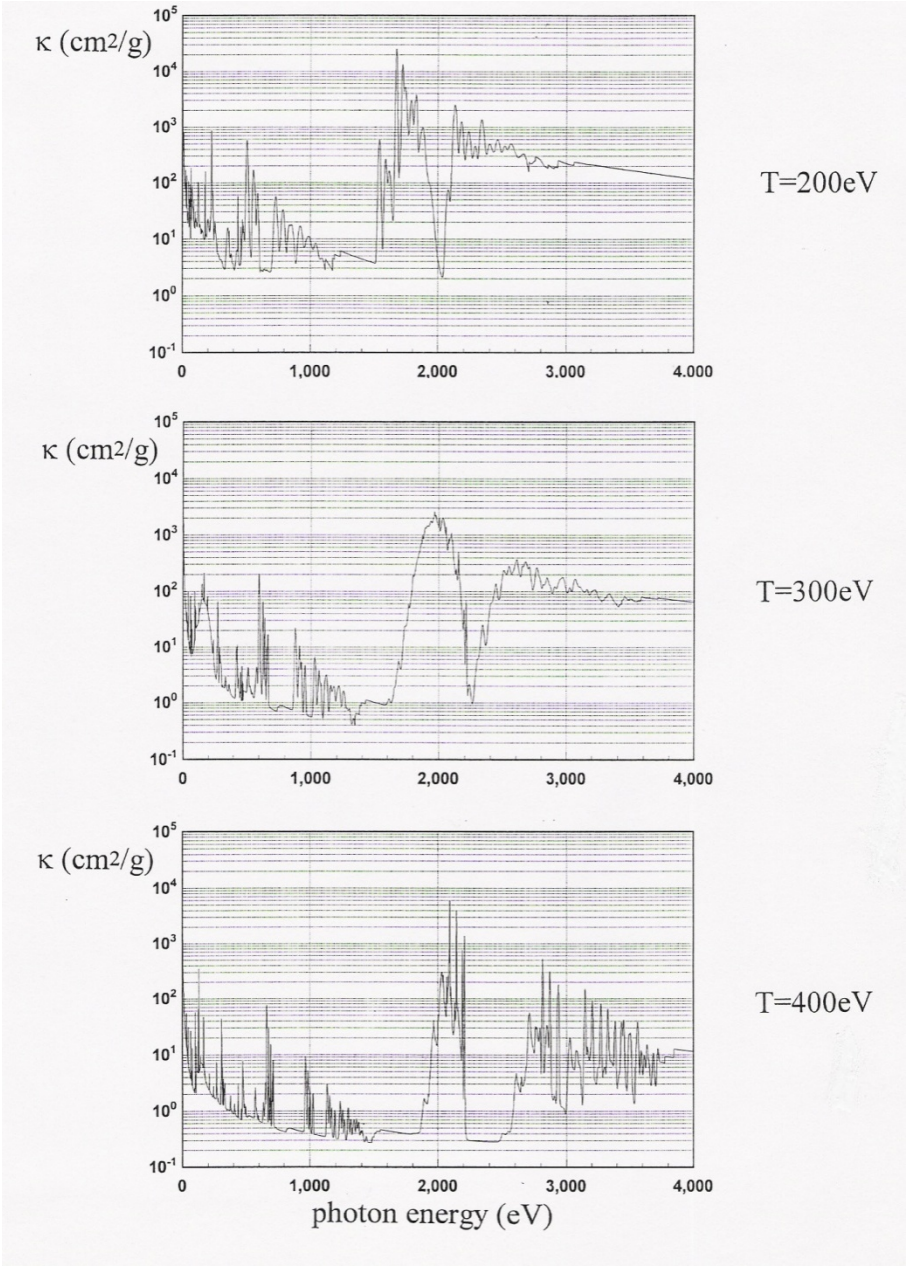

Comparison between theory and experiment

Narrow-band radiation field

Line-coincidence photopumping

Simplified diagram of the Bowen resonance fluorescence mechanism

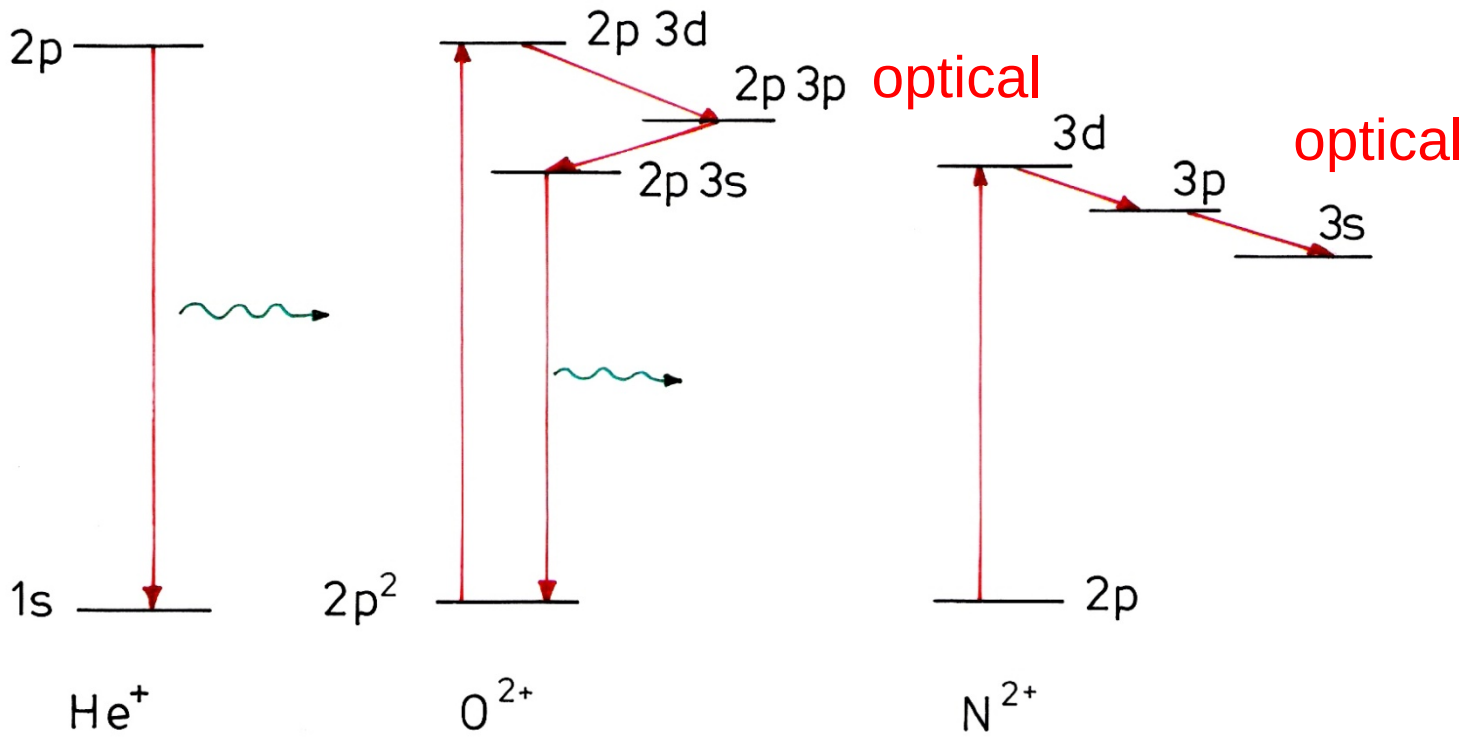

Bowen, Publ. Astr. Soc. Pac.(1934)

Astrophysical line-coincidence photopumping and lasing

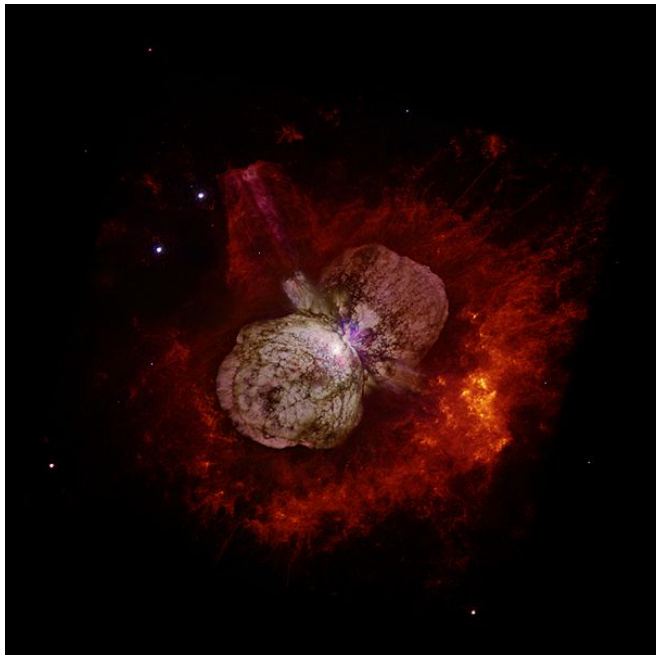

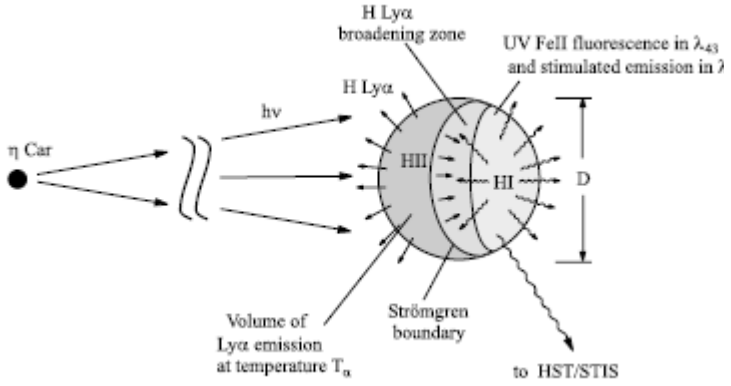

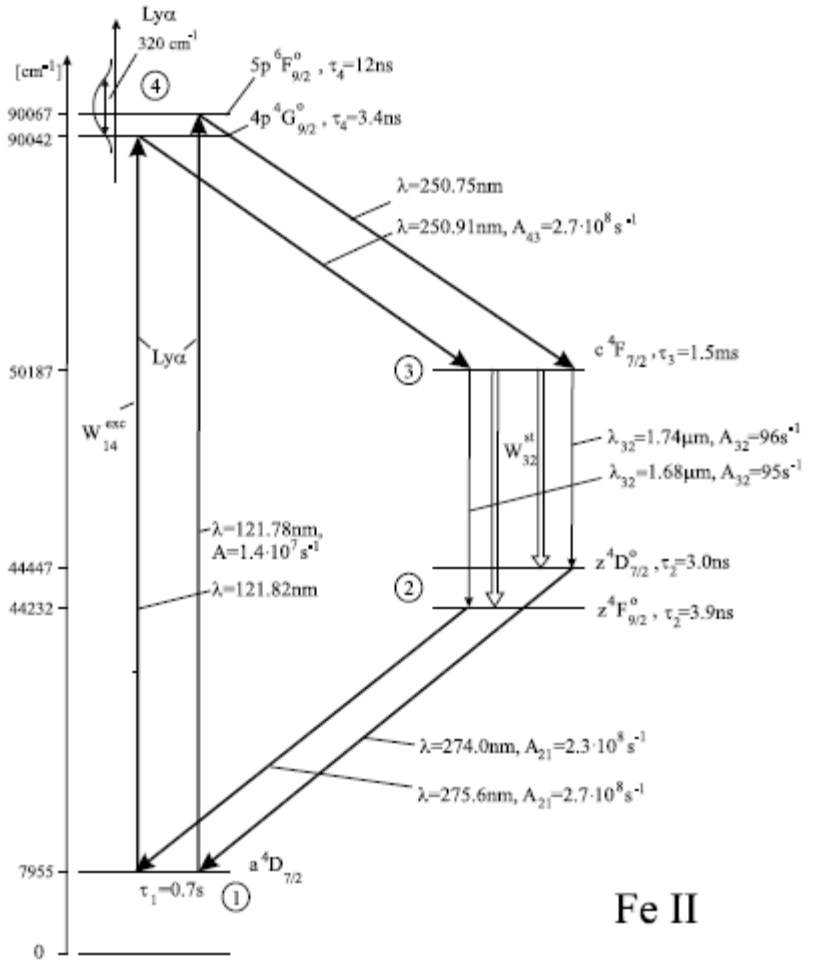

Johanssen and Letokhov,, Astrophysical Lasers, CUP (2009)

Accidental line coincidences H-like and He-like ions

Table 1. Possible X-ray laser schemes.

Si 2^1P_1(1864.9 eV)	+	Al 3^3P_1(ΔE = 1.0 eV)
		3^1P_1(ΔE = 3.8 eV)
Mn $2P_{3/2}$(6441.4 eV)	+	V 4^1P_1(ΔE = −2.6 eV)
		4^3P_1(ΔE = −5.4 eV)
Fe 2^3P_1(6667.3 eV)	+	Cr 3^3P_1(ΔE = 5.6 eV)
Ge $2P_{1/2}$(10574.9 eV)	+	Zn 3^3P_1(ΔE = −0.3 eV)
Se 2^3P_1(14567.4 eV)	+	Br 3^3P_1(ΔE = −2.1 eV)
Pd $2P_{3/2}$(22372.7 eV)	+	Mo 4^1P_1(ΔE = −3.6 eV)

Alley, Chapline, Kunasz and Weisheit, JQSRT(1982)

Calculation of line coincidences

Na $1s^2\,{}^1S_0 - 1s2p\,{}^1P_1 \rightarrow$ Ne $1s^2\,{}^1S_0 - 1s4p\,{}^1P_1$	E(Na; $1s^2\,{}^1S_0 - 1s2p\,{}^1P_1$) - E(Ne; $1s^2\,{}^1S_0 - 1s4p\,{}^1P_1$)
Dirac-Fock SCF	0.11eV
Dirac-Fock SCF + Breit	-0.01eV
Dirac-Fock SCF + Breit +QED	-0.06eV
Experiment	-0.25eV

Transition energies ~ 1.13keV

Sr $1s^2\,{}^1S_0 - 1s2p\,{}^3P_1 \rightarrow$ Br $1s^2\,{}^1S_0 - 1s3p\,{}^1P_1$	E(Sr; $1s^2\,{}^1S_0 - 1s2p\,{}^3P_1$) - E(Br; $1s^2\,{}^1S_0 - 1s3p\,{}^1P_1$)
Dirac-Fock SCF	9.0eV
Dirac-Fock SCF + Breit	5.1eV
Dirac-Fock SCF + Breit +QED	1.9eV
Dirac-Fock SCF + Breit +QED + finite nucleus	1.7eV

Transition energies ~ 14.6keV

Rose, JQSRT(1985)

H-like and He-like K / H-like Cl line-coincidence photopumping

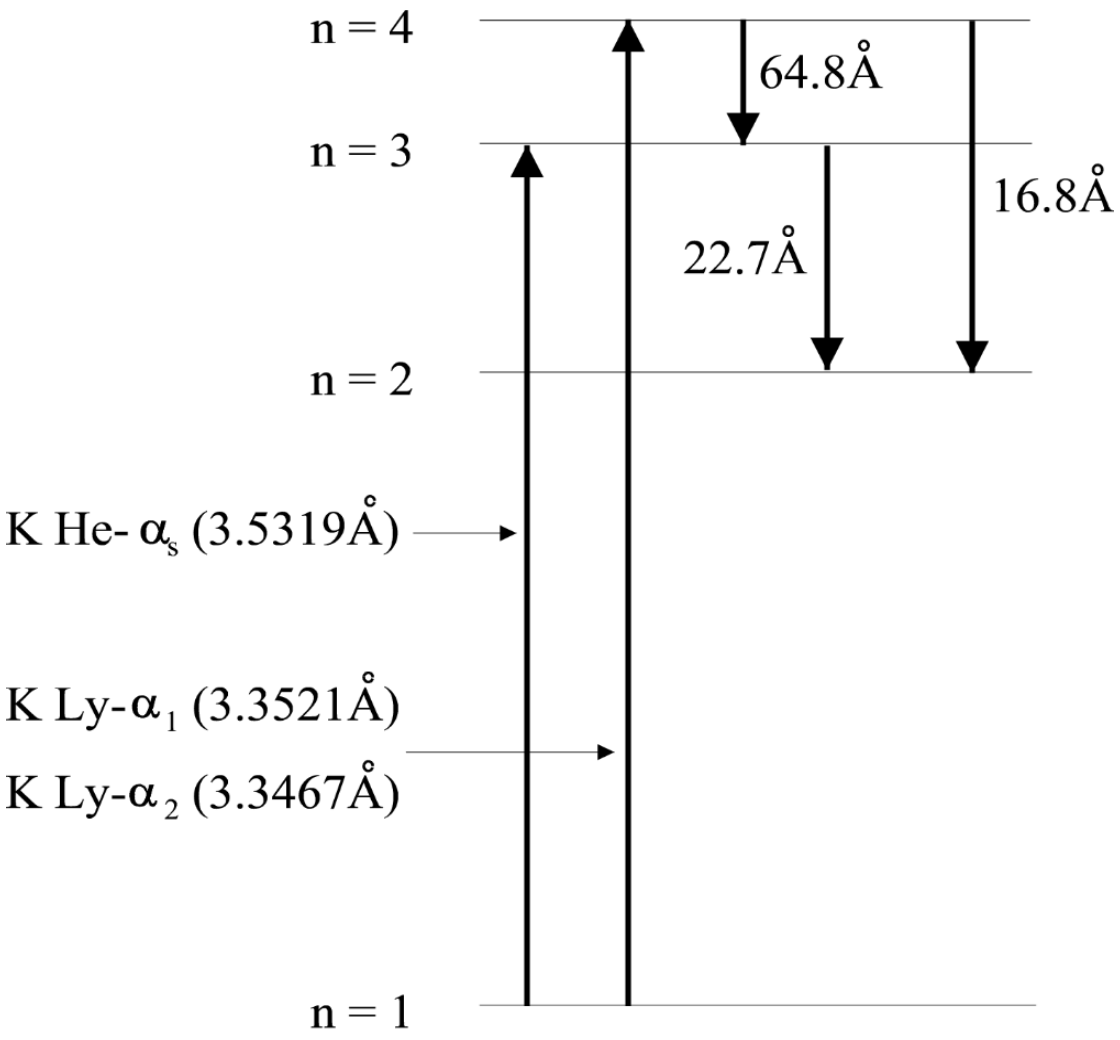

Line coincidence photopumping in a laboratory plasma

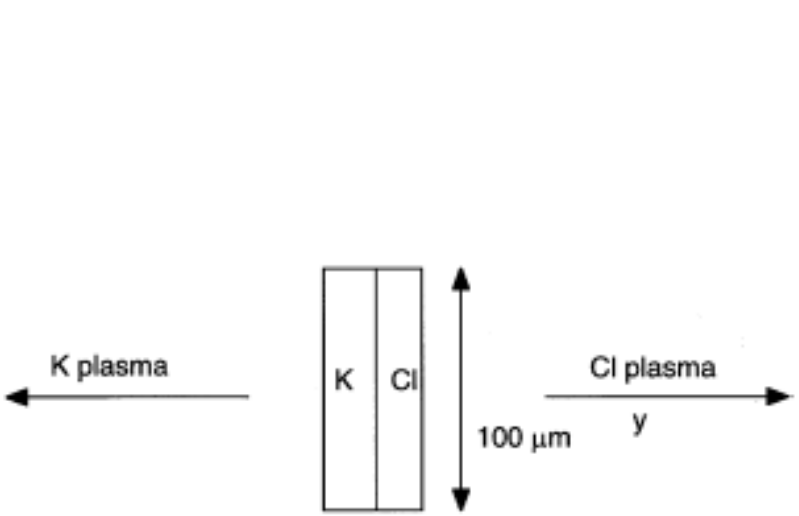

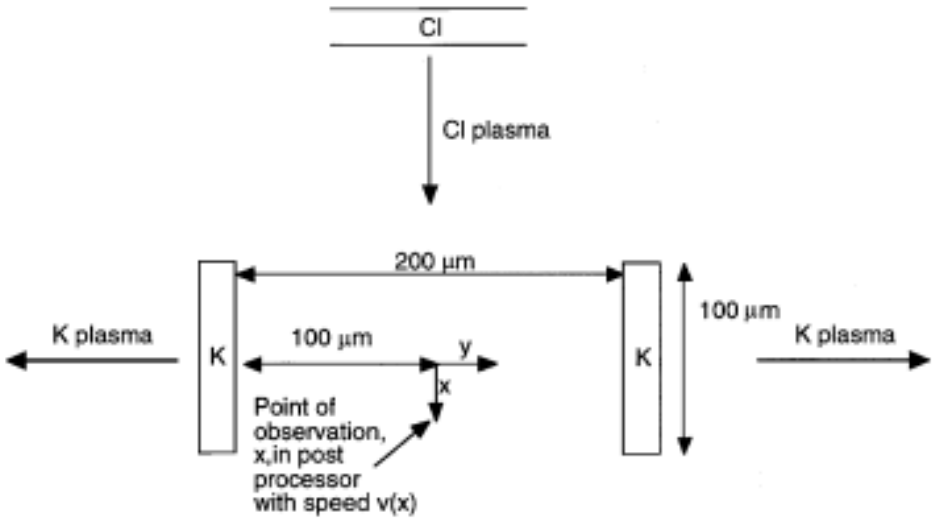

Beer, Patel, Rose and Wark, JQSRT (2000)

Line coincidence photopumping in a laboratory plasma

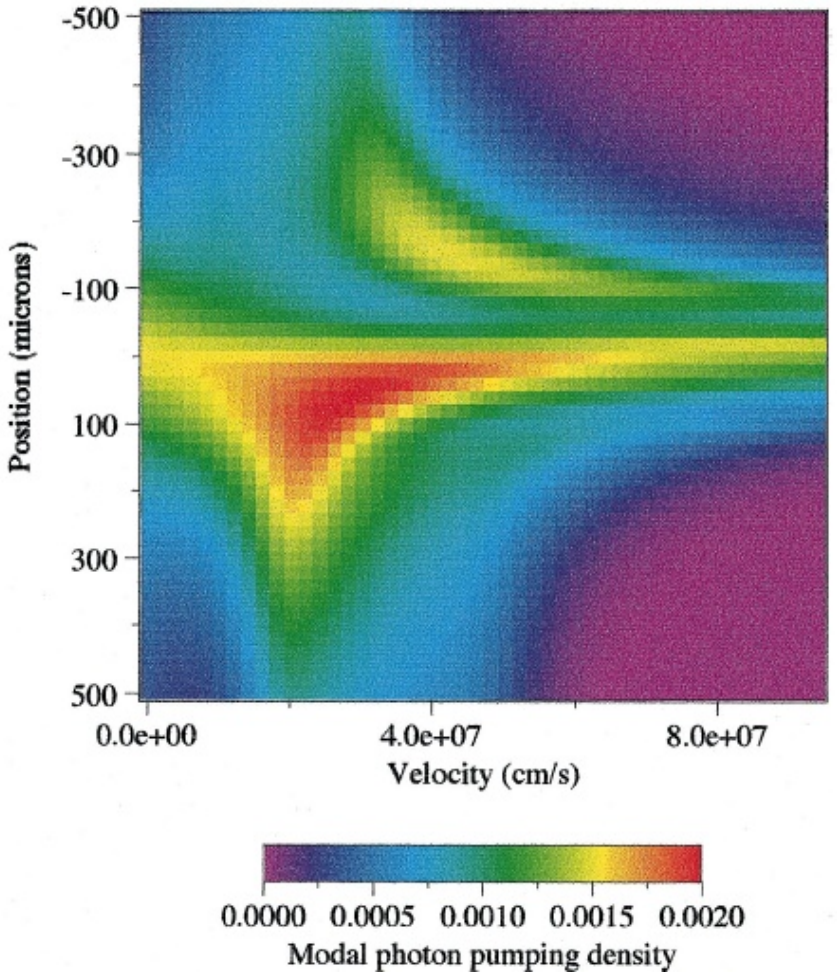

Modal photon density n_{ph} in the frame of the Cl ions at 3.3507Å (Cl $1s_{1/2} – 4p_{3/2}$) at distance x and velocity v(x) at the peak of the laser pulse.

Beer, Patel, Rose and Wark, JQSRT (2000)

Line radiation transport in a velocity gradient

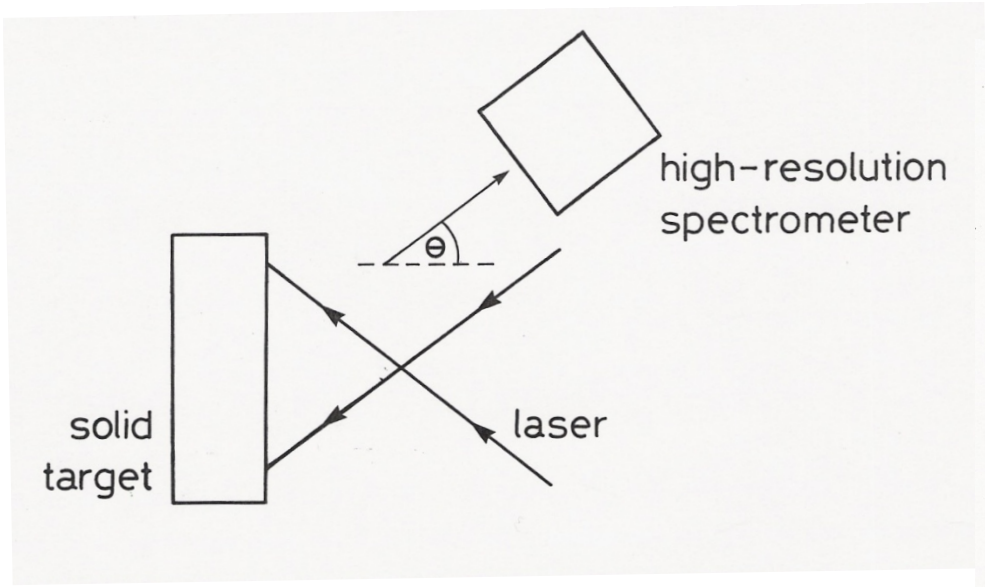

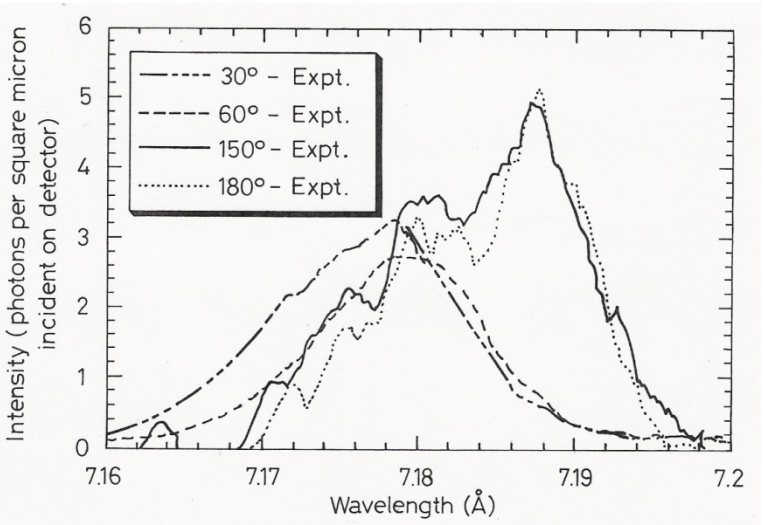

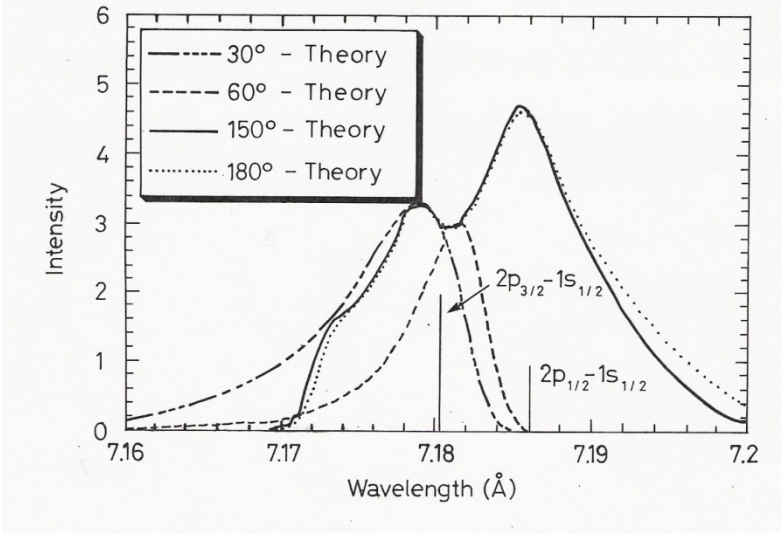

Wark, Djaoui, Rose, He, Renner, Missalla, Foerster, Physical Review Letters (1994)

Line radiation transport in a velocity gradient

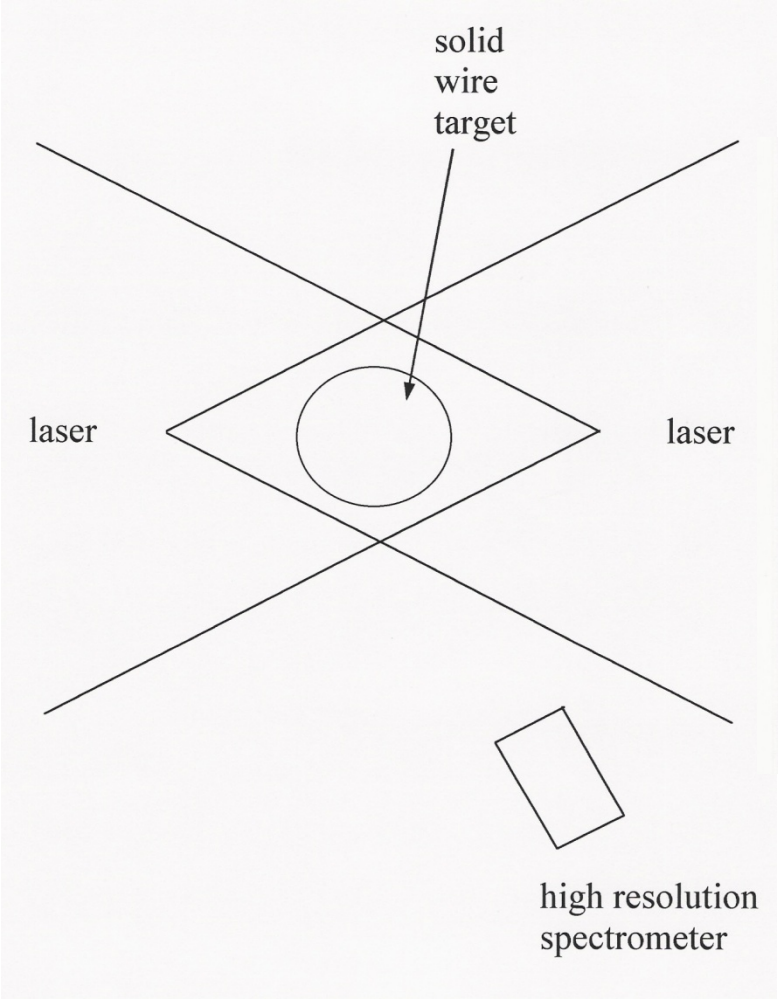

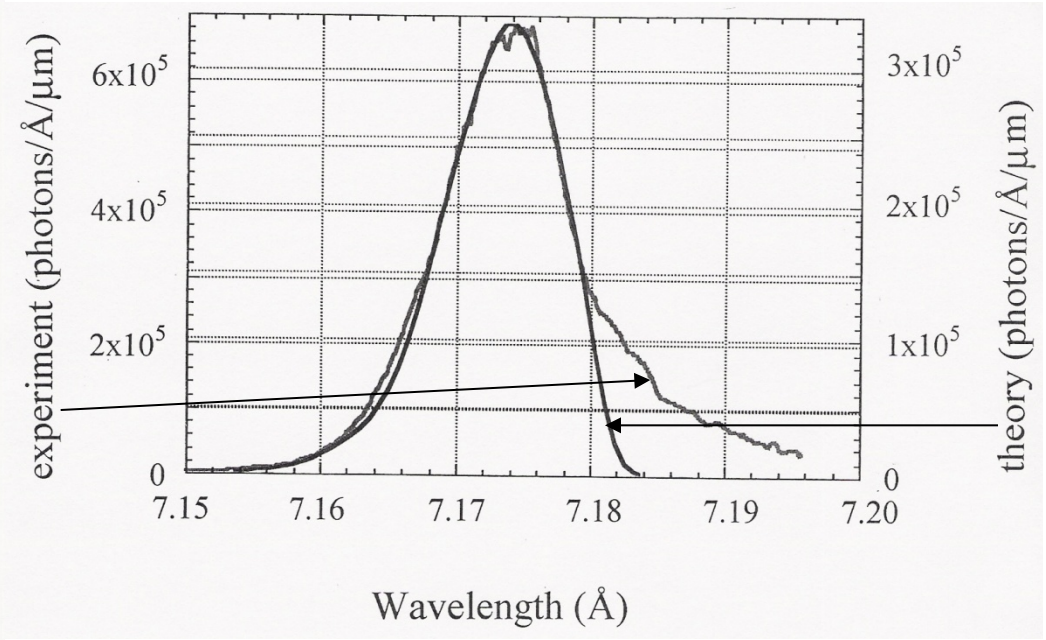

Patel, Wark, Renner, Djaoui, Rose, Heading, Hauer, JQSRT (1997)

Experimental evidence for XUV/X-ray line-coincidence photopumping

There are only a few experiments in which line-coincidence photopumping has been demonstrated in the XUV / X-ray range through measurement of *enhanced fluorescence*:

Monier et (1988) Al/Si

Back et al (1991) Al/Al

O'Neill et al (1990) Mn/F

Gouveia et al (2003) Al/Fe

One experiment has measured *population inversion:*

Porter et al (1992) Na/Ne

There is no experimental evidence for *lasing* in the XUV or X-ray range through line-coincidence photopumping.

Na / Ne line coincidence photopumping scheme

Na $1s^2\,{}^1S_0 - 1s2p\,{}^1P_1$

Ne

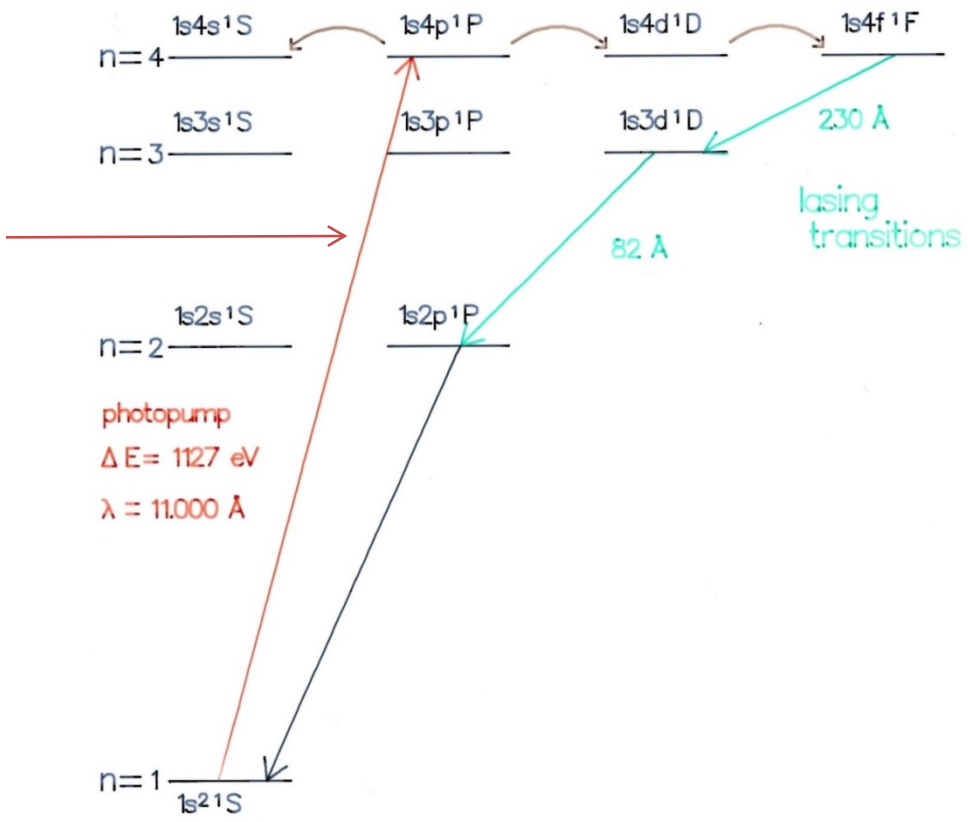

Porter et al, Phys Rev Letts (1992)

Na / Ne line coincidence photopumping scheme

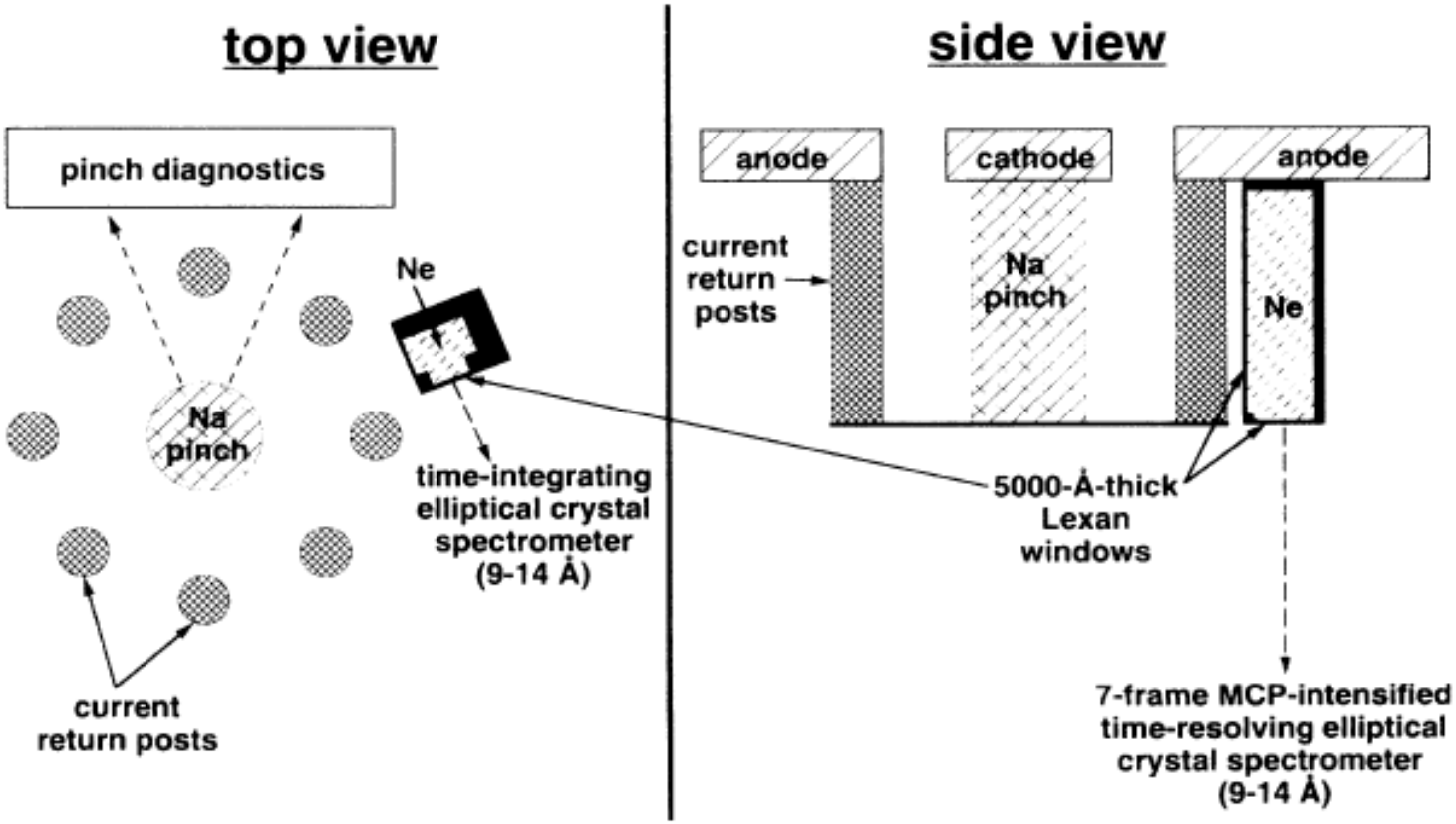

Population inversion measured

Porter et al, Phys Rev Letts (1992)

Proposed astrophysical line coincidence photopumping

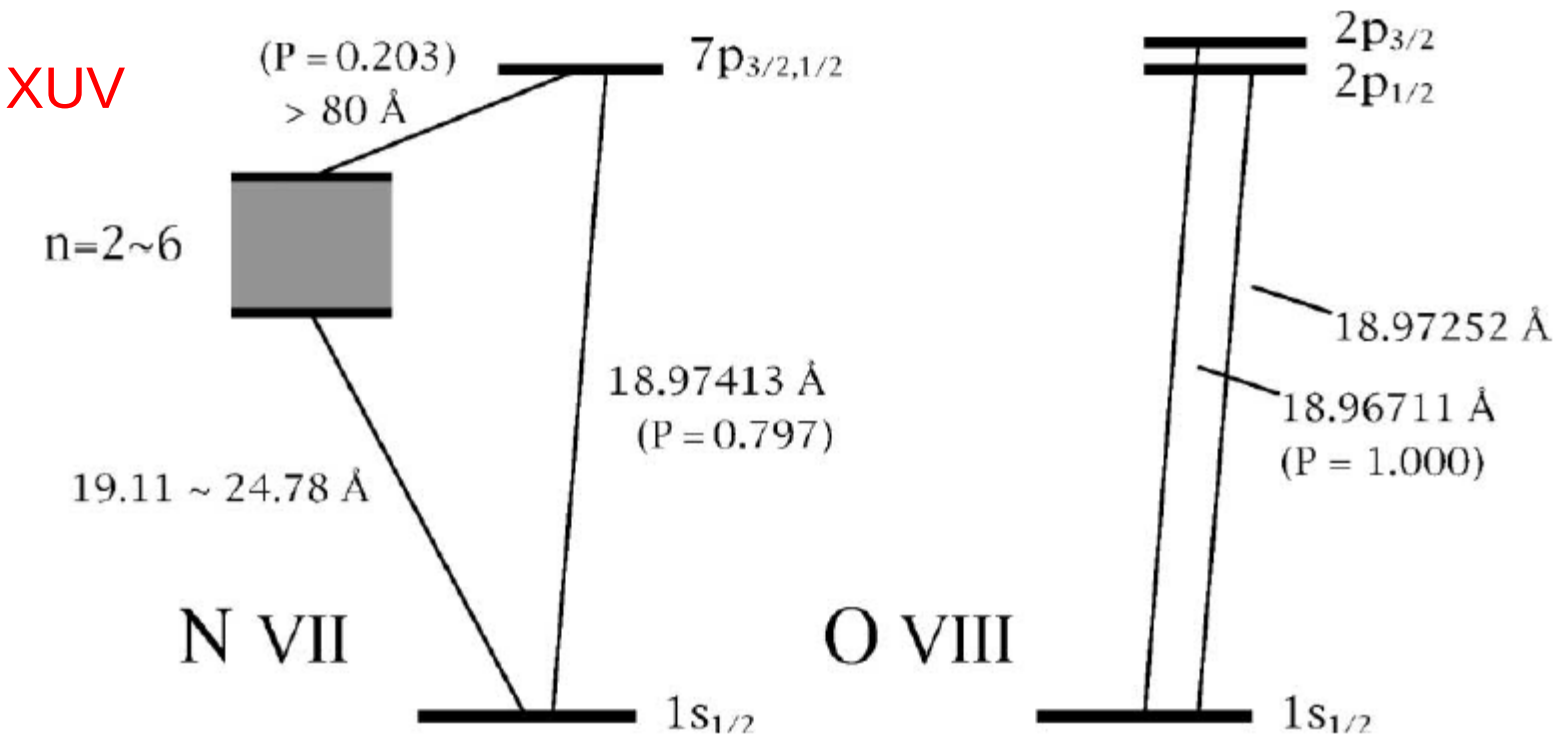

Sako et al, ApJ (2003)

Na / Ne line coincidence photopumping astrophysical scheme

H / He / Ne / Na plasma with astrophysical Ne and Na abundances (0.68637 / 0.3113 / 1.3831×10^{-4} / 2.9461×10^{-6})

Na / Ne line coincidence photopumping astrophysical scheme

H / He / Ne / Na plasma with astrophysical Ne and Na abundances (0.68637 / 0.3113 / 1.3831×10^{-4} / 2.9461×10^{-6})

$n_e = 10^{10}$-10^{13} cm^{-3}

$l = 10^{9} – 10^{13}$ cm

$T_e = 100 – 200$ eV

Internal ‘Bowen’ pumping of lines by accidental line-coincidence

The radiative excitation and de-excitation rates for the pumped ion are:

$$R^r_{\alpha\to\beta} = A_{\beta\to\alpha} n_{ph} \left(\Omega_\beta / \Omega_\alpha\right)$$

$$R^r_{\beta\to\alpha} = A_{\beta\to\alpha} (1 + n_{ph})$$

$$n_{ph} = \frac{1}{\frac{n_\chi \Omega_\delta}{n_\delta \Omega_\chi} - 1}$$

‘Bowen’ pumping of transition
$\alpha \to \beta$ by $\chi \leftrightarrow \delta$
(Judge, MNRAS,1988)

Rose, JPhysB (1998)

Na / Ne line coincidence photopumping laboratory scheme

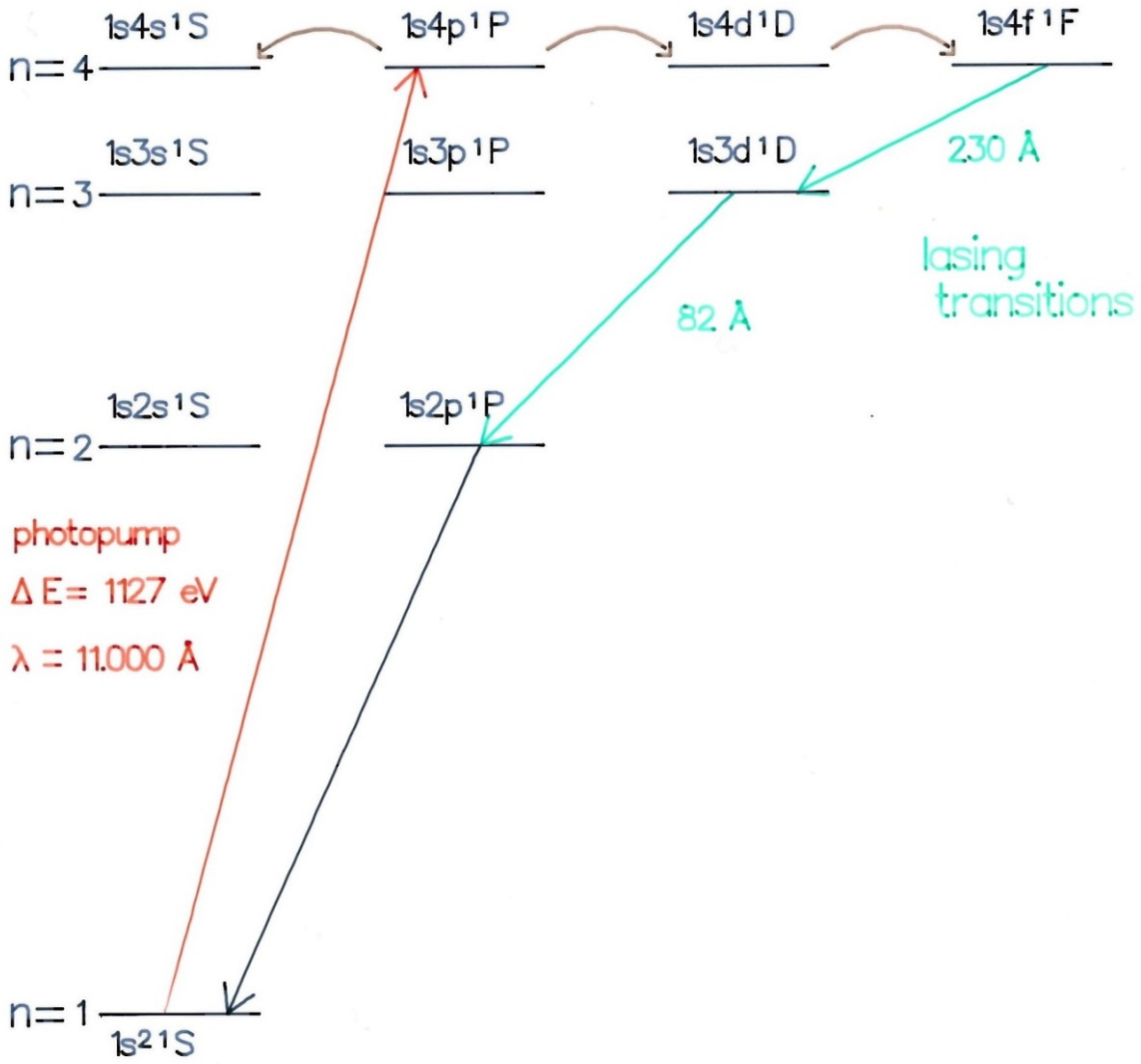

Porter et al, Phys Rev Letts (1992)

Na / Ne line coincidence photopumping astrophysical scheme

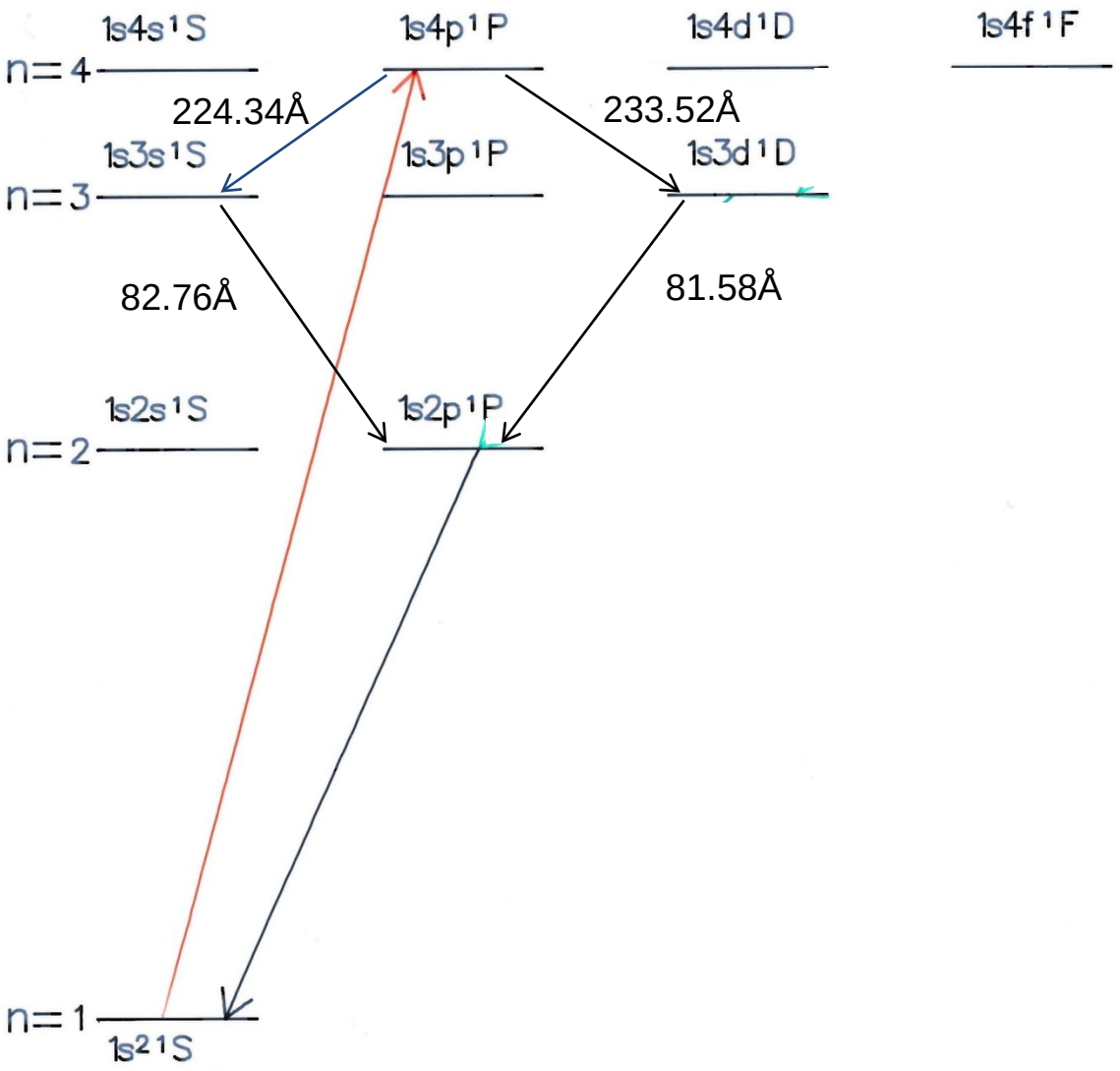

Keenan et al, MNRAS (2018)

Spectroscopy of the Sun

On July 13th 1982 a rocket-borne spectrograph that measured the 10 - 100Å emission from an M-class flare on the Sun with 0.02Å resolution.

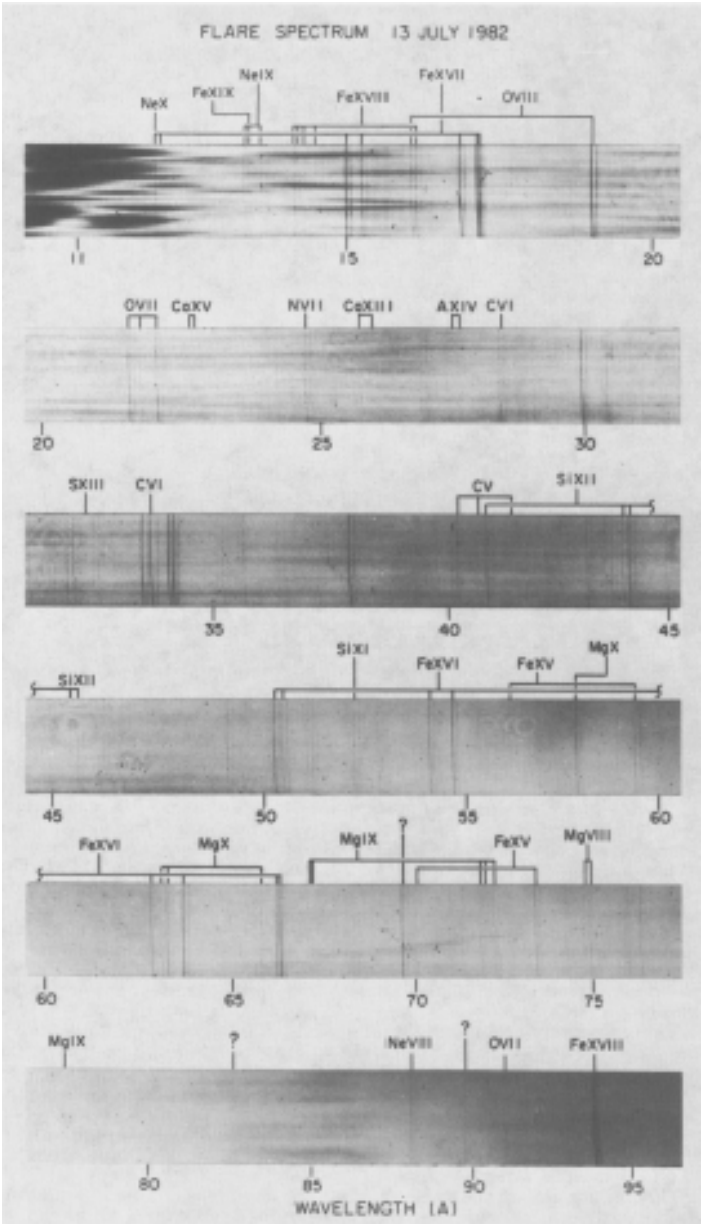

Acton et al, Ap J (1985)

Na / Ne line coincidence photopumping astrophysical scheme

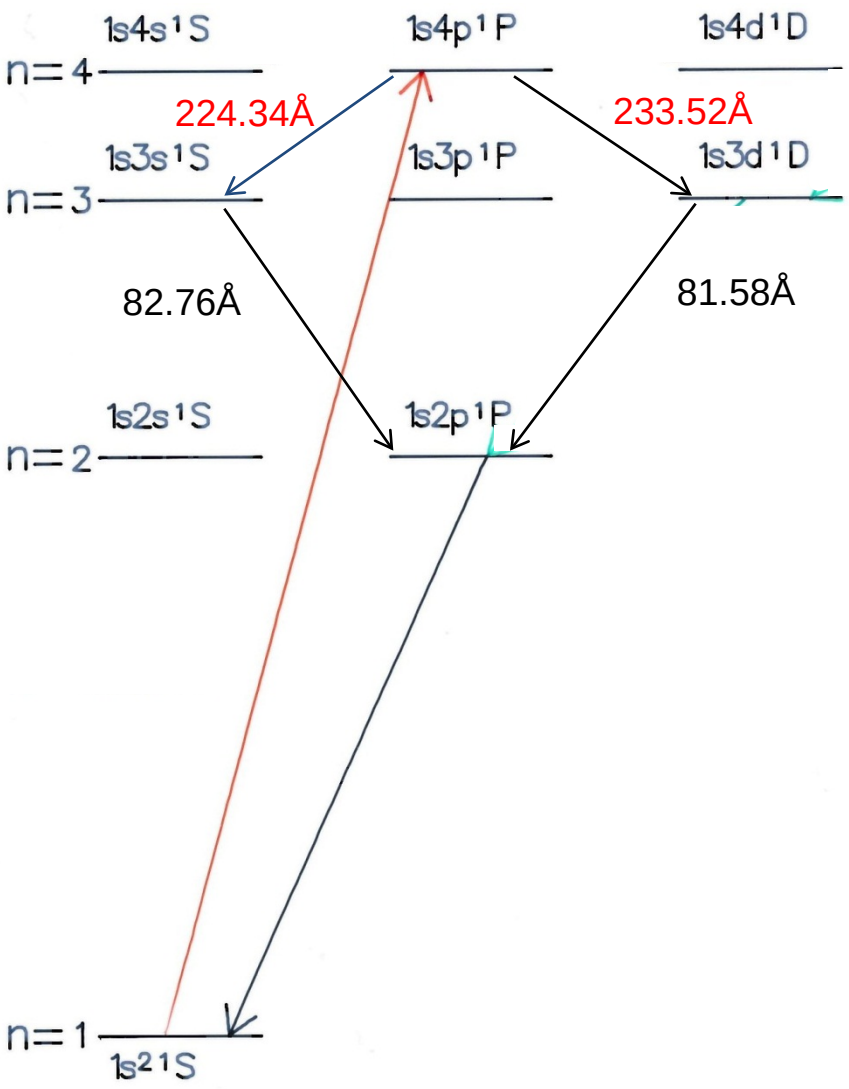

In solar flare spectra, the NeIX 224.34Å and 233.52Å lines are blended with the strong FeXIV 224.35Å and OIV 233.55Å features.

Keenan et al, MNRAS (2018)

Na / Ne line coincidence photopumping astrophysical scheme

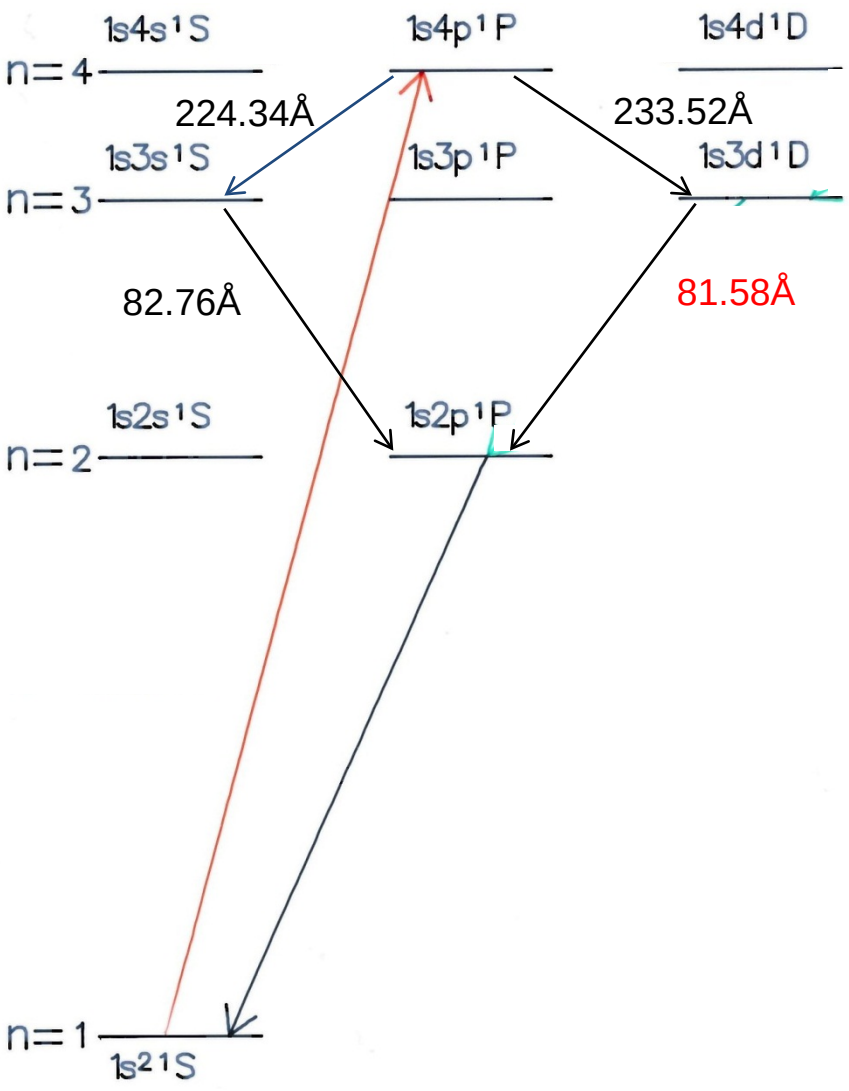

NeIX 81.58Å line has predicted enhancement which is too small even under optimal conditions to detect the feature.

Keenan et al, MNRAS (2018)

Na / Ne line coincidence photopumping astrophysical scheme

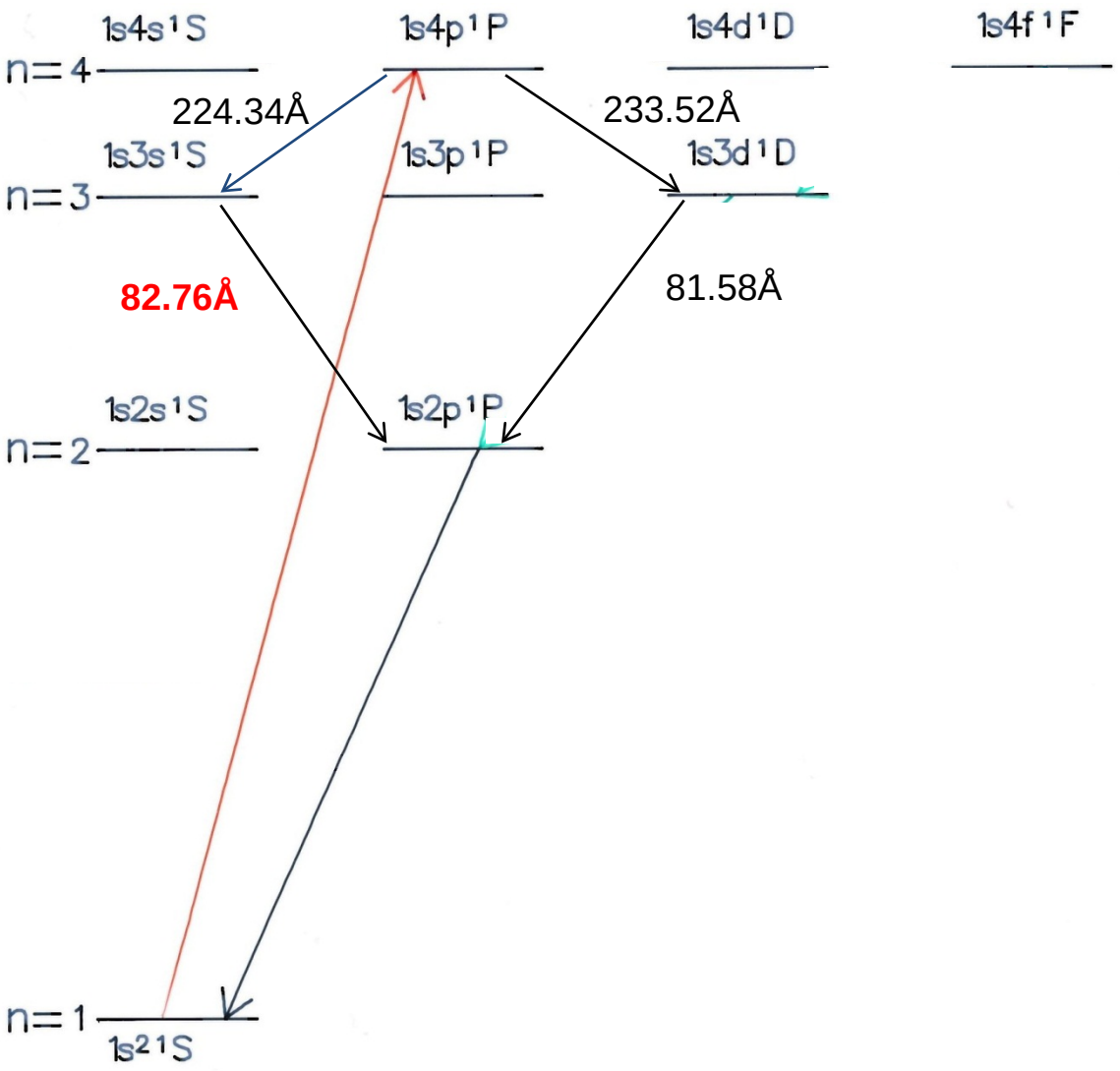

Keenan et al, MNRAS (2018)

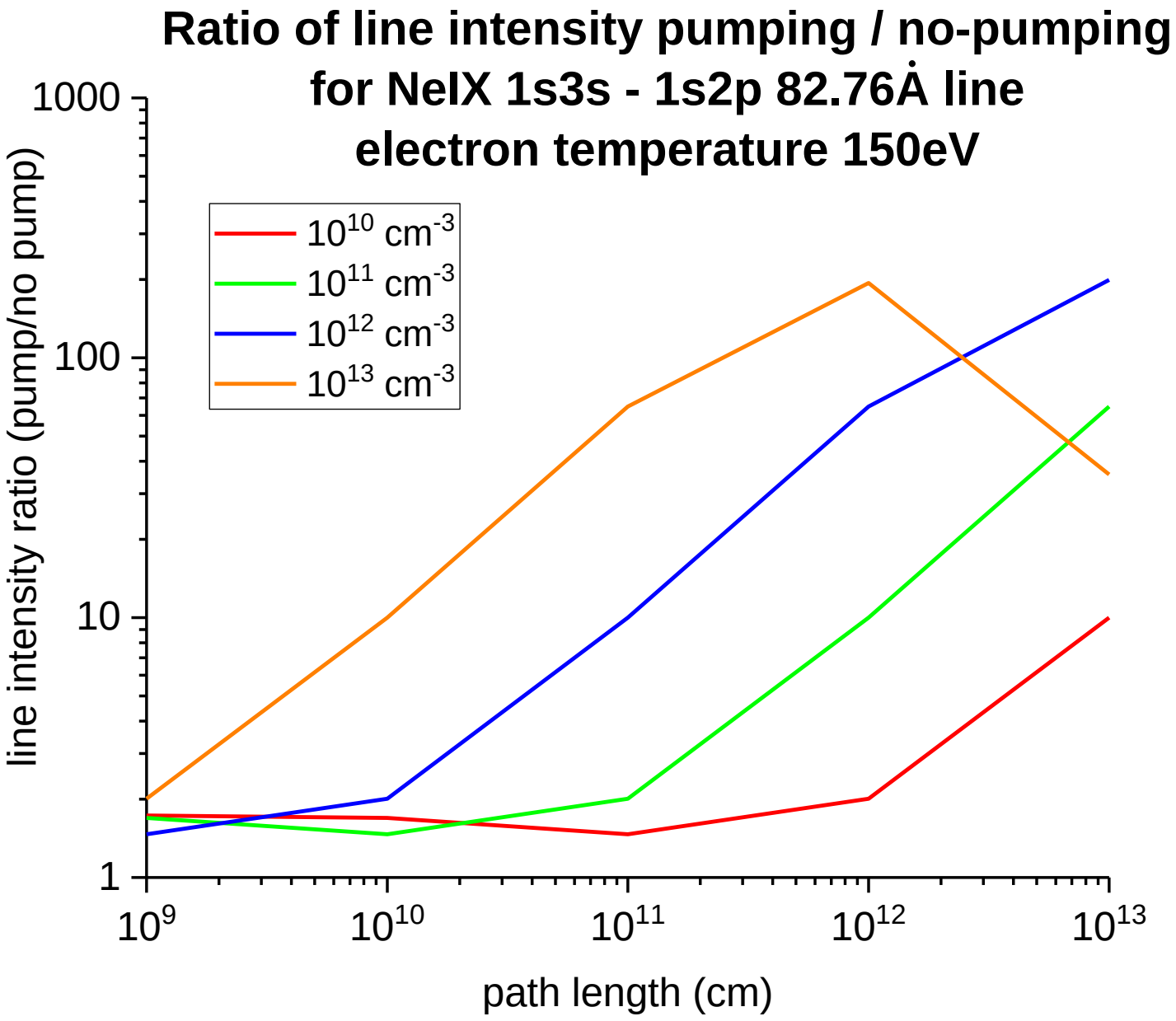

Keenan et al, MNRAS (2018)

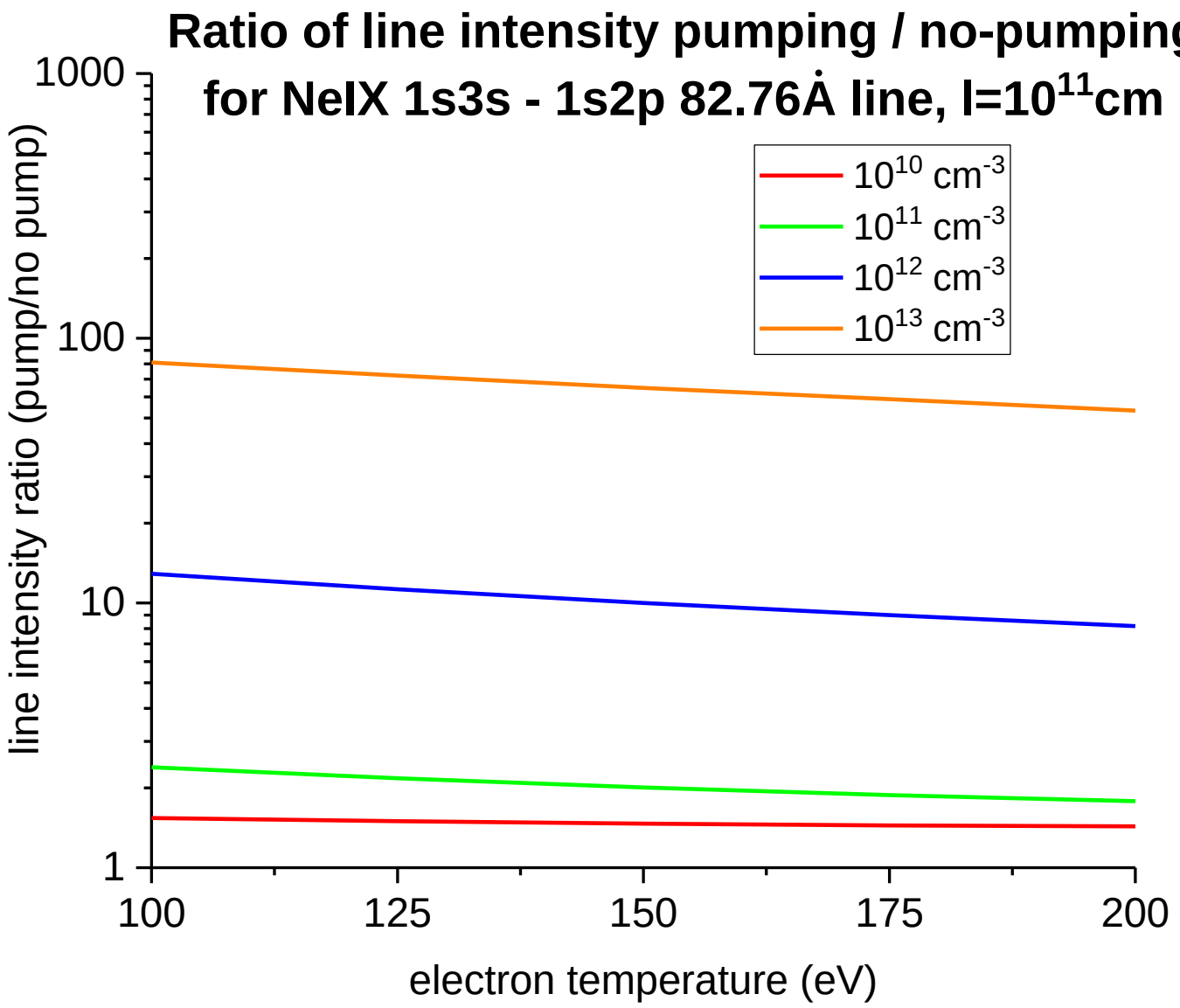

Keenan et al, MNRAS (2018)

CHIANTI modelling of the spectroscopy of the Sun

- CHIANTI gives the electron density of the flare to be $n_e = 10^{11} cm^{-3}$.

- CHIANTI gives the electron temperature of the flare to be 150eV.

- CHIANTI predicts that in the absence of photopumping, the 82.76Å line feature is at least 50% NeIX 1s3s $^1S_1$ – 1s2p $^1P_1$ with the other intensity arising from Fe transitions.

- Maximum flare loop length is about 10^{10}cm (Shibata and Magara 2011).

Keenan et al, MNRAS (2018) Dere et al, Astron Astrophys Suppl (1997), Del Zanna et al, Astron Astrophys (2015)

CHIANTI modelling of the spectroscopy of the Sun

- CHIANTI analysis predicts line intensity ratios (in photon units) with NeIX lines at 13.45 and 13.70 to be 82.76/13.45 = 0.019 and 82.76/13.70 = 0.020, compared to measured values of 0.20 and 0.24, respectively.

- These imply enhancements in in 82.76Å line intensity of about a factor of 5.

- CHIANTI analysis predicts line intensity ratios (in photon units) with Fe XV and Fe XVI lines at 73.47A and 76.80A to be 82.76/73.47 = 0.16 and 82.76/76.80 = 0.30, compared to measured values of 0.52 and 0.19, respectively.

- These imply enhancements in 82.76Å line intensity of factors of 3.25 and 1.6 respectively.

Keenan et al, MNRAS (2018)

Acton et al, Ap J (1985)

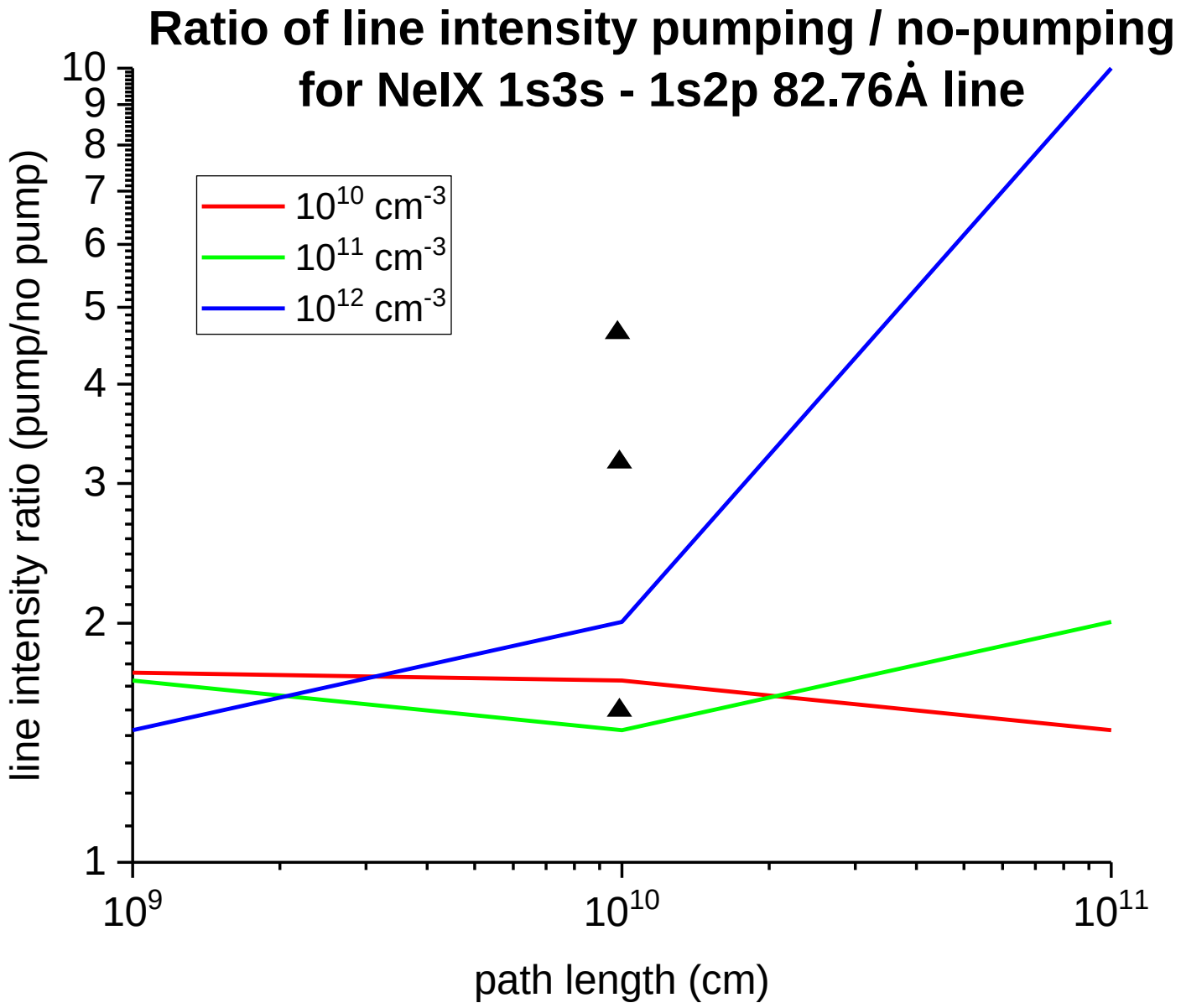

Keenan et al, MNRAS (2018)

XUV photopumping in the Sun's corona

- First tentative evidence for X-ray line coincidence photopumping in an astrophysical source.

- However the evidence must be treated with some caution:

  The flare spectrum was recorded on photographic film and is no longer accessible and hence the quality of the 82.76Å line measurement (and indeed those of other transitions) cannot be confirmed.

  The 13.45Å and 13.70Å and the 82.76Å features lie close to opposite ends of the flare wavelength coverage (10 – 100Å), so that instrument sensitivity calibration may be an issue.

- We would like to extend our observations to CHANDRA satellite data – access to database required.

- We have started a programme of experiments on the ORION laser to test our modelling of internal 'Bowen' line-coincidence photopumping.

Conclusions

The theory of direct excitation and ionisation by an ambient radiation field is well established.

The modelling involves atomic data and coverage uncertainties.

Comparison between experiment and theory even for no radiation field shows differences.

Broad-band pumping experiments show reasonable agreement with theory.

Narrow-band pumping experiments show poor agreement with theory, although there is fairly good agreement in line radiation transfer.

This is an area in which modelling still has a long way to go.